

UNCLASSIFIED



Australian Government
Department of Defence
Defence Science and
Technology Organisation

The Characterisation of a PEM Fuel-Cell System with a Focus on UAS Applications

James R. Harvey and Jennifer L. Palmer

Aerospace Division
Defence Science and Technology Organisation

DSTO-TR-2934

ABSTRACT

Under DSTO's Strategic Research Initiative on Signatures, Materials, and Energy, a project entitled "Hybrid-Propulsion and Power-Management Technologies for Tactical Unmanned Aircraft Systems (UAS)" is underway. Fuel cells have been identified as having the potential to substantially increase the range and endurance of small, electrically-powered fixed-wing aircraft. Herein described are experiments conducted on a Hy-Expert Instructor Fuel Cell System, aimed at developing fundamental knowledge of polymer-electrolyte membrane fuel-cell characteristics and the methodology used to characterise fuel-cell systems. Given the focus of future work, emphasis was placed on issues relevant to UAS applications.

RELEASE LIMITATION

Approved for public release

UNCLASSIFIED

UNCLASSIFIED

Published by

*Aerospace Division
DSTO Defence Science and Technology Organisation
506 Lorimer St
Fishermans Bend, Victoria 3207 Australia*

*Telephone: 1300 333 362
Fax: (03) 9626 7999*

*© Commonwealth of Australia 2014
AR-015-844
January 2014*

APPROVED FOR PUBLIC RELEASE

UNCLASSIFIED

UNCLASSIFIED

The Characterisation of a PEM Fuel-Cell System with a Focus on UAS Applications

Executive Summary

Under DSTO's Strategic Research Initiative on Signatures, Materials, and Energy, a project entitled "Hybrid-Propulsion and Power-Management Technologies for Tactical Unmanned Aircraft Systems (UAS)" is underway. Because their specific energy (energy per unit mass) is usually superior to that of comparable powerplants, fuel cells have the potential to greatly increase the range and endurance of small, tactical UAS. Herein, the authors developed fundamental knowledge of polymer-electrolyte membrane (PEM) fuel cells through experiments conducted on a commercially available system: the Hy-Expert Instructor Fuel Cell System. Given the focus of future work, emphasis was placed on issues relevant to UAS applications.

In this report, the fundamental principles of PEM fuel-cell technology are outlined; and the fuel cell's driving chemical reactions, physical structure, and behaviour under load are described. Also provided are the results of experiments conducted to determine the voltage, power, and efficiency characteristics of the Hy-Expert stack, as well as its fuel consumption under a varying load. The thermal and water management of the fuel-cell stack and the parasitic loads imposed by the fuel cell's balance of plant (*i.e.*, cooling and air-supply fans and control electronics) are also described.

Although the Hy-Expert system documented in this report exhibits similar characteristics to larger systems, it is not suitable for UAS applications. However, the experiments described here provide valuable insight into the fundamental mechanisms of PEM fuel-cell operation and various issues relevant to UAS applications. For example, irreversibilities inherent to fuel-cell stacks create a dependence of output voltage on load current; and this poses a significant issue for implementing a fuel cell onto an aircraft, which has devices on-board requiring fixed voltage(s). A voltage converter or some additional fixed-voltage source, such as a battery, is needed to power electrical loads requiring constant input voltages, such as payloads, avionics, communications equipment, and the devices required to control and provide reactants for the fuel-cell stack. The presence of such devices, including a voltage regulator or an additional power source, however, will incur additional electrical losses and add mass to the aircraft.

Finally, an example of basic fuel-cell design for a small UAS is presented. The analysis illustrates how to make use of equations describing the characteristics of fuel cells to roughly size a fuel-cell stack and the reactant requirements for a typical UAS mission.

UNCLASSIFIED

UNCLASSIFIED

Authors

Mr. James Harvey Aerospace Division



James Harvey graduated from the University of Adelaide with first-class honours in Mechatronic Engineering in 2009. There his final year project involved the development of an autonomous unmanned aerial system (UAS) for search and rescue missions. He joined DSTO in Air Vehicles Division in 2010 where he has conducted research into hybrid-electric power systems for all-electric tactical UAS and on developing experimental techniques for characterising flapping-wing micro air vehicle (MAV) aerodynamics.

Dr. Jennifer L. Palmer Aerospace Division



Dr. Palmer joined the Defence Science & Technology Organisation in 2007, as a member of the Air Vehicles Division. Her current work focuses on unmanned aircraft, including projects on hybrid-propulsion and power-management technologies for small surveillance aircraft and flapping-wing flight. Prior to immigrating to Australia from the US in 2004, she was employed at Lockheed Martin Missiles & Space in Sunnyvale, California, where her work involved analyses of missile systems and test failures. She earned a Ph.D. in Mechanical Engineering from Stanford University in 1997, with a thesis on the demonstration of advanced laser-based diagnostic techniques for hypersonic flows.

UNCLASSIFIED

Contents

LIST OF FIGURES

LIST OF TABLES

GLOSSARY

1. INTRODUCTION.....	1
1.1 Overview and Background	1
1.2 Aim	4
2. FUNDAMENTAL PEM FUEL-CELL OPERATION	5
2.1 The Driving Chemical Reaction.....	5
2.2 Physical Structure	5
2.2.1 Polymer-Electrolyte Membrane	6
2.2.2 Electrodes	6
2.2.3 Bipolar Plates	6
2.3 Voltage Response.....	6
2.3.1 Activation Over-Voltage	7
2.3.2 Fuel Crossover and Internal Currents	8
2.3.3 Ohmic losses.....	8
2.3.4 Concentration Losses	8
3. SYSTEM OVERVIEW	9
3.1 Specifications of the Hy-Expert Fuel Cell	9
3.2 Voltage and Power Response	9
3.2.1 Voltage- and Power-Current Characteristic Curves	10
3.2.2 Determination of Ohmic Losses	12
4. SYSTEM EFFICIENCIES	13
4.1 Stack Efficiency	15
4.2 Voltage and Current Efficiencies	16
4.3 Alternative Methods of Calculating Efficiency	18
5. REACTANT SUPPLY AND THERMAL MANAGEMENT	19
5.1 Hydrogen Supply.....	19
5.1.1 Hydrogen Flow Rate <i>vs.</i> Load Current	19
5.1.2 Hydrogen Storage	20
5.2 Air Supply	21
5.2.1 Fuel-Cell Performance with Restricted Airflow	21
5.2.2 Required Airflow Rate.....	22
5.2.3 Supply of Oxygen.....	23

5.3	Thermal Management	24
5.3.1	Effect of Operating Temperature	24
5.3.2	Alternative Methods for Thermal Management.....	24
6.	POWER SUPPLY	27
6.1	Parasitic Load	27
6.2	Voltage-Conversion Losses	28
6.3	Power-Supply Efficiency	30
6.3.1	Total Efficiency	31
6.3.2	Stack and System Efficiency.....	31
7.	CONCEPTUAL FUEL-CELL-SYSTEM DESIGN	33
7.1	Stack Size	33
7.2	Reactant Requirements	33
7.2.1	Hydrogen Flow Rate	33
7.2.2	Oxygen-Flow and Airflow Rates.....	34
8.	CONCLUSION	35
	REFERENCES	37
	ACKNOWLEDGEMENTS	46
	APPENDIX A: WORK HEALTH AND SAFETY DOCUMENTS	47

List of Figures

1	(a) Wingspan and (b) wing loading as functions of maximum take-off mass for battery- and fuel-cell-powered aircraft. The fuel-cell UAVs represented are: the 0.065-kg MITE [22-24]; 0.17-kg Hornet [12, 15, 25, 26]; 1.9-kg solid-oxide-fuel-cell- (SOFC-) powered UAV [6, 27]; 2.5-kg KAIST UAV [28, 29]; 2.6-kg Hy-Fly [30-32]; 3.1-kg Spider Lion [24, 33-35]; 5.3-kg SOFC UAV [6, 27, 36]; 5.4-kg Puma [15, 20, 21]; 6.0-kg HyFish [37, 38]; 6.5-kg EAV-1 [14-17]; 7.7-kg FAUCON H2 [39, 40]; 9.0-kg Boomerang/EAV-1 [15, 18, 19]; 13-kg Pterosoar [41-43]; 16-kg Ion Tiger [15]; 16-kg GTRI Demonstrator [5, 32, 44-48]; 79-kg Global Observer prototype Odyssey [15, 49-53]. References [9, 54-83] provide the displayed data for manned aircraft.	2
2	Aircraft flight endurance as a function of maximum take-off mass for battery- and fuel-cell-powered aircraft, with the differences between the demonstrated (actual) and potential endurance of several fuel-cell-powered UAVs highlighted. The same UAVs and manned aircraft represented in Figure 1 are shown, where endurance data is available.	3
3	Photograph of the Heliocentris Hy-Expert Instructor Fuel Cell System and a laptop computer that can be used to control its variable load and to record data from the system. Photograph reprinted from [85].	4
4	The basic operation of a single PEM hydrogen fuel cell.....	5
5	Schematic of a generic PEM fuel-cell stack.....	6
6	A typical fuel-cell voltage-current curve, where the stack voltage falls below the ideal no-loss voltage with increasing stack current.....	7
7	Hy-Expert system in grid-dependent mode, in which the grid powers the BOP devices, including fans, valves, LEDs, <i>etc.</i>	10
8	(a) Voltage-current curve and (b) power-current curve for the Hy-Expert stack	11
9	Equivalent circuit representing internal resistances in the Hy-Expert system.....	13
10	Voltage-current characteristic curves, measured across the stack (V_{stack}) and at the output terminals (V_{term})	13
11	Hydrogen flow rate as a function of stack current for the Hy-Expert system.....	15
12	Stack efficiency and power as functions of stack current for the Hy-Expert system	16
13	Voltage, current, and stack efficiencies of the Hy-Expert fuel cell	17

14	Hy-Expert voltage response under normal and reduced-airflow conditions.....	22
15	Hy-Expert power response under normal and reduced-air conditions	23
16	Voltage-current characteristic curves for initial stack temperatures of 28 and 44 °C	25
17	Layout of the Hy-Expert system in grid-independent mode, where the stack provides a variable voltage to the output load and a fixed voltage to the BOP devices	27
18	(a) Parasitic load and (b) output-load and stack power as functions of stack current when the Hy-Expert system is operated in grid-independent mode.....	29
19	Layout of the Hy-Expert system in grid-independent mode, with the stack providing a fixed voltage to the output load and BOP devices.....	30
20	Output-load power as a function of current with and without voltage converter in the circuit	30
21	Total efficiency as a function of output-load power.....	31
22	Stack and system efficiencies as functions of output-load power	32

List of Tables

1 Hy-Expert stack specifications [86]	9
2 Parasitic-load and stack power under no-load conditions, when the Hy-Expert system is operated in grid-independent mode.....	28

UNCLASSIFIED

DSTO-TR-2934

This page is intentionally blank

UNCLASSIFIED

Glossary

Acronyms

BOP	Balance of plant
GDL	Gas-diffusion layer
GTOM	Gross take-off mass
GTRI	Georgia Technology Research Institute
HHV	Higher heating value
KAIST	Korea Advanced Institute of Science and Technology
LED	Light-emitting diode
LHV	Lower heating value
MITE	Micro Tactical Expendable
NRL	(US) National Research Laboratory
PEM	Polymer-electrolyte membrane
SOFC	Solid-oxide fuel cell
UAS	Unmanned aircraft system or systems
UAV	Unmanned air vehicle

Symbols

A	Active surface area of each cell (cm^2)
B	Boron
e^-	Electron
f_{H_2}	Fraction of hydrogen flow rate not lost to fuel crossover
\mathcal{F}	Faraday's constant, $9.648 \times 10^4 \text{ C/g-mol}$
H^+	Hydrogen ion
H_2	Molecular hydrogen
H_2O	Molecular water
HHV	Higher heating value of H_2 , 12.8 MJ/m^3 at standard conditions
I	Load current (A)
I_{stack}	Stack current (A)
$I_{stack,max}$	Maximum stack current (A)
I_{th}	Current theoretically produced for a given hydrogen flow rate (A)
LHV	Lower heating value of H_2 , 10.8 MJ/m^3 at standard conditions
Li	Lithium
m_{stack}	Stack mass (kg)
M	Unspecified metallic substance
MH_2	Molecule composed of a metallic substance and a hydrogen molecule
Na	Atomic sodium
$NaBH_4$	Sodium borohydride molecule
$NaBO_2$	Sodium borate molecule
n	Amount of a substance (g-mol)
$no.cells$	Number of cells in stack
O_2	Oxygen molecule
P_{BOP}	Power consumed by BOP devices (W)
$P_{ext,loss}$	Power losses associated with the Ohmic losses external to the stack (W)

P_{in}	Power input to the stack (W)
P_{out}	Power output from the fuel-cell system (W)
P_{stack}	Stack power (W)
$P_{stack,loss}$	Power losses associated with the Ohmic losses within the stack (W)
$P_{stack,max}$	Maximum fuel-cell power (W)
R_{addl}	Internal resistances external to the stack (Ω)
R_{stack}	Internal resistances within the stack (Ω)
R_{tot}	Total system internal resistance (Ω)
V_{cell}	Cell voltage (V)
V_o	Current source (V)
$V_{rev,LHV}$	Reversible thermodynamic voltage at the LHV, 1.25 V for hydrogen
$V_{rev,HHV}$	Reversible thermodynamic voltage at the HHV, 1.48 V for hydrogen
V_{stack}	Stack voltage (V)
V_{term}	Voltage across the variable output load (V)
V_{rev}^0	Free-reaction enthalpy, 1.23 V for hydrogen
\mathcal{V}_{air}	Total volume of air (ℓ)
\mathcal{V}_{H_2}	Total volume of H_2 (ℓ)
\mathcal{V}_m	Molecular standard volume, 22.4 ℓ /g-mol
\mathcal{V}_{O_2}	Total volume of O_2 (ℓ)
$\mathcal{V}_{air}^{\dot{}}$	Volumetric airflow rate (ℓ /min)
$\mathcal{V}_{H_2}^{\dot{}}$	Volumetric rate of flow of H_2 (ℓ /min)
$\mathcal{V}_{H_2,act}^{\dot{}}$	Actual (measured) volumetric rate of flow of H_2 (ℓ /min)
$\mathcal{V}_{H_2,th}^{\dot{}}$	Volumetric rate of flow of H_2 theoretically required to produce a given stack current (ℓ /min)
z_{H_2}	Valency of a hydrogen ion, $2 e^-$ /ion
z_{H_2O}	Valency of a hydrogen ion, $2 e^-$ /ion
z_{O_2}	Valency of an oxygen ion, $4 e^-$ /ion
Δg_f	Gibbs free energy of H_2 , 10.6 MJ/m ³ at standard conditions
ΔI_{stack}	Increase in stack current for a given increase in hydrogen flow rate (A)
$\Delta \mathcal{V}_{H_2}^{\dot{}}$	Increase in hydrogen flow rate for a given increase in stack current (ℓ /min)
ρ_{cell}	Current density (A/cm ²)
ρ_p	Specific power of the stack (W/kg)
λ	Ratio of excess air provided to fuel cell
η_1	Current efficiency
η_{stack}	Stack efficiency
η_{sys}	System efficiency
η_V	Voltage efficiency

Units

A	Amperes
C	Coulombs
°C	Degrees Celsius
cm	Centimetres
g-mol	Gram-moles
h	Hours
kg	Kilograms

km	Kilometres
kPa	Kilopascals
<i>ℓ</i>	Litres
m	Metres
min	Minutes
<i>mℓ</i>	Millilitres
MJ	Megajoules
N	Newtons
V	Volts
W	Watts
Ω	Ohms

This page is intentionally blank

1. Introduction

1.1 Overview and Background

Under DSTO's Strategic Research Initiative on Signatures, Materials, and Energy, a project on "Hybrid-Propulsion and Power-Management Technologies for Tactical Unmanned Aircraft Systems (UAS)" is underway. The research is focussed on technologies and operating strategies that can significantly extend the range and endurance of small, electrically powered, fixed-wing aircraft. Fuel-cell systems have the potential to greatly increase the energy stored on-board small aircraft, compared with that available from batteries. Thus compact fuel-cell systems are of interest. Herein described is a laboratory characterisation of a commercially available polymer-electrolyte membrane (PEM) fuel cell: the Hy-Expert™ Instructor Fuel Cell System. Given the focus of future work, emphasis is placed on issues relevant to UAS applications.

Fuel cells have a higher fuel efficiency (defined as energy output divided by energy input as fuel) than do internal combustion engines; and they are mechanically simpler, with few or no moving parts [1, 2]. They produce low acoustic and thermal signatures, which are desirable for military applications; and they are generally environmentally friendly, with water as the predominant by-product when hydrogen is the fuel [1-3]. The primary advantage of fuel cells over lithium-based (*Li*) batteries is their higher specific energy (Wh/kg), which provides the potential for greater aircraft endurance over more conventional, battery-powered aircraft. However, in comparison to *Li* batteries, fuel cells exhibit relatively low specific power (W/kg) [3-6]. This has stimulated the development of hybrid systems that utilise a combination of battery and fuel-cell technologies [6-11].

Several successful flights of fuel-cell-powered UAS have been performed by research groups and commercial organisations around the world [1, 12]. Figure 1 displays the essential physical characteristics of various electrically powered manned aircraft and unmanned air vehicles (UAVs), gathered from the open literature [13]. The wingspan of each is shown as a function of its maximum gross take-off mass (GTOM) in Figure 1(a); and the wing loading (mass per unit wing area) of each aircraft, where available, is shown in Figure 1(b). A comparison of the data for aircraft powered by batteries with that for aircraft powered by fuel cells indicates that the latter tend to have slightly larger wingspans at the same GTOM, though these simple measures and the limited dataset for wing loading do not reveal marked differences in their designs. Indeed, many of the fuel-cell-powered aircraft identified in Figure 1 are battery-powered designs adapted to carry fuel cells.

The impact of replacing a battery pack with a fuel-cell system is illustrated in Figure 2, where the flight endurance achievable for specific aircraft with *Li*-polymer or -primary batteries is compared with the endurance achieved (or potentially achievable) with a fuel cell in the same aircraft. The plot indicates results obtained in several recent demonstrations of fuel-cell-powered flight performed with existing, commercially available UAS designs, including Uconsystem's Remo Eye 006 [14-17], BlueBird's Boomerang [15, 18, 19], and Aerovironment's Puma [15, 20, 21].

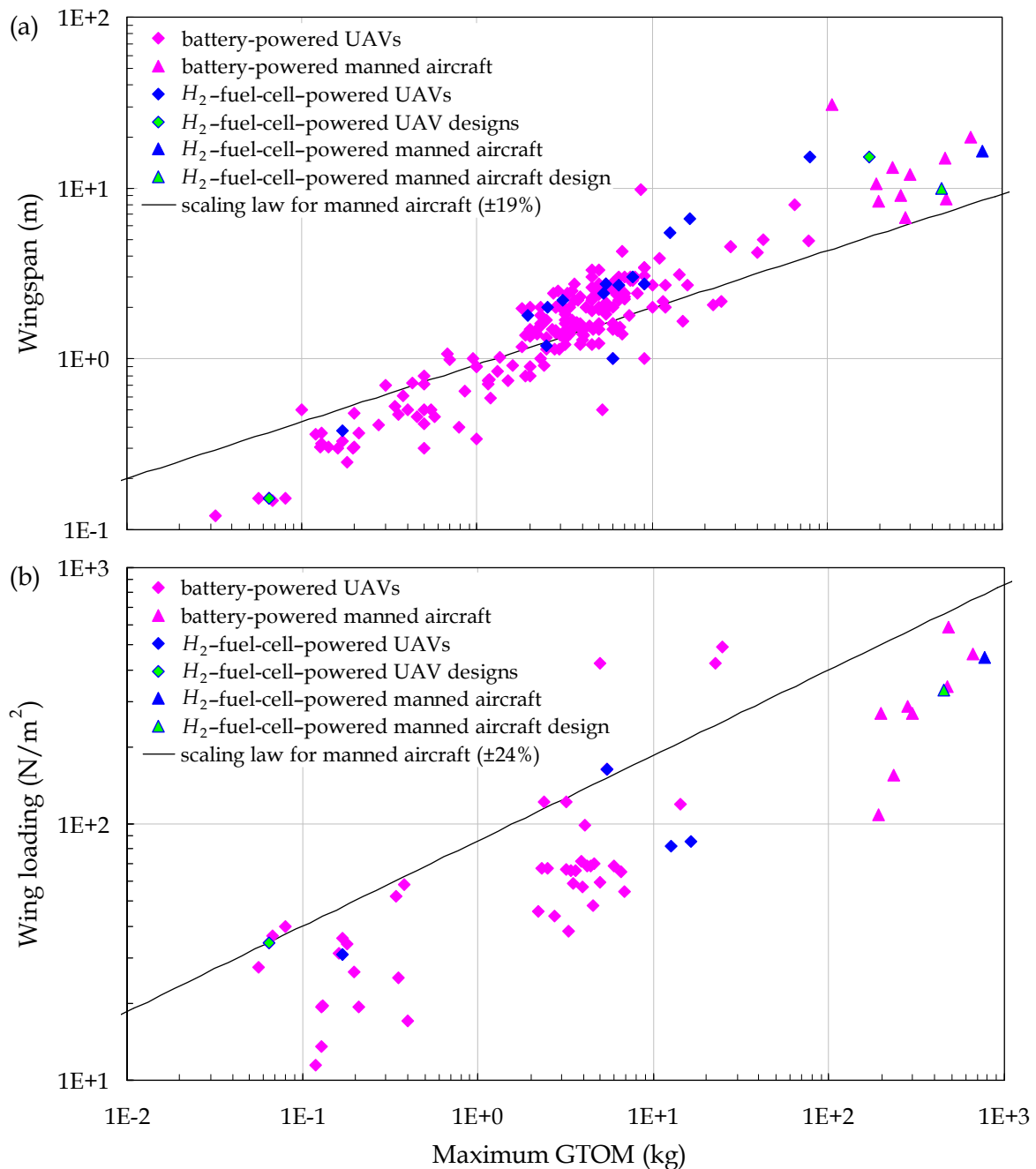


Figure 1 (a) Wingspan and (b) wing loading as functions of maximum take-off mass for battery- and fuel-cell-powered aircraft. The fuel-cell UAVs represented are: the 0.065-kg MITE [22-24]; 0.17-kg Hornet [12, 15, 25, 26]; 1.9-kg solid-oxide-fuel-cell- (SOFC-) powered UAV [6, 27]; 2.5-kg KAIST UAV [28, 29]; 2.6-kg Hy-Fly [30-32]; 3.1-kg Spider Lion [24, 33-35]; 5.3-kg SOFC UAV [6, 27, 36]; 5.4-kg Puma [15, 20, 21]; 6.0-kg HyFish [37, 38]; 6.5-kg EAV-1 [14-17]; 7.7-kg FAUCON H2 [39, 40]; 9.0-kg Boomerang/EAV-1 [15, 18, 19]; 13-kg Pterosoar [41-43]; 16-kg Ion Tiger [15]; 16-kg GTRI Demonstrator [5, 32, 44-48]; 79-kg Global Observer prototype Odyssey [15, 49-53]. References [9, 54-83] provide the displayed data for manned aircraft.

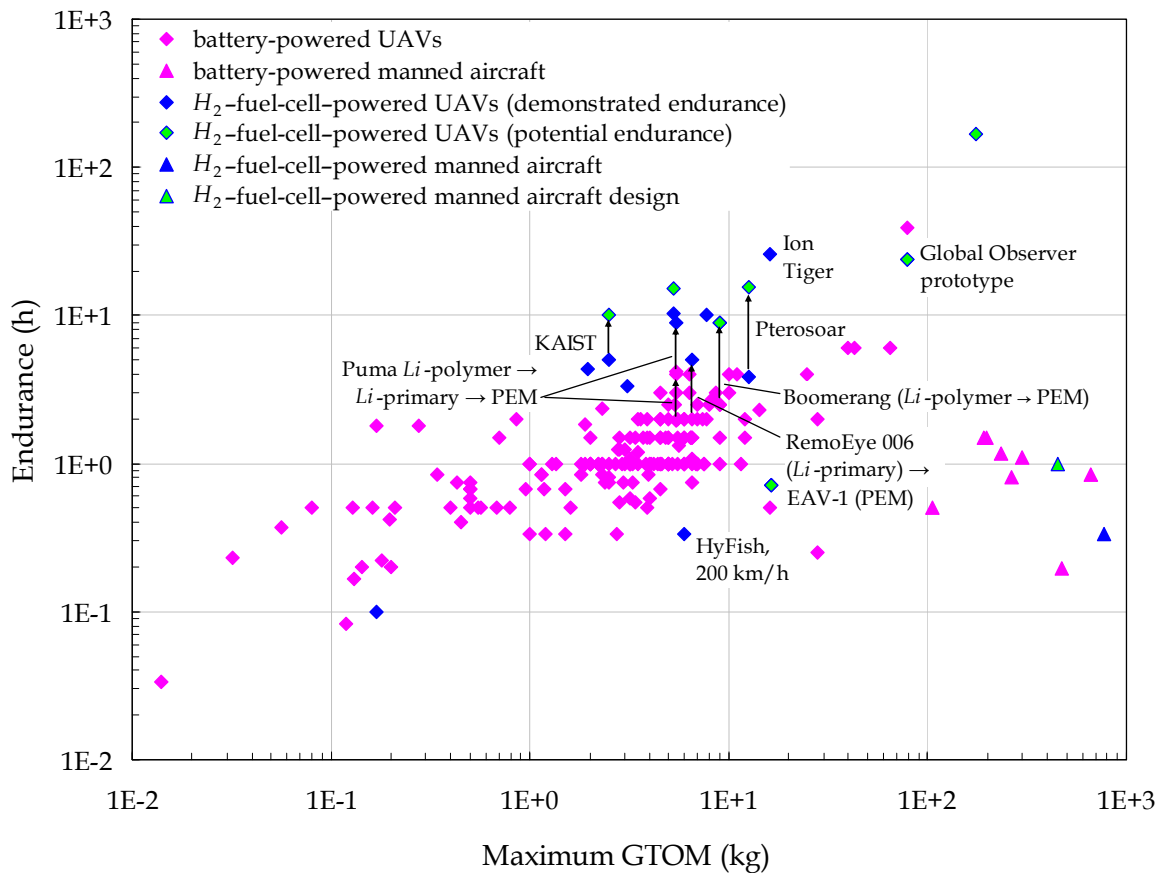


Figure 2 Aircraft flight endurance as a function of maximum take-off mass for battery- and fuel-cell-powered aircraft, with the differences between the demonstrated (actual) and potential endurance of several fuel-cell-powered UAVs highlighted. The same UAVs and manned aircraft represented in Figure 1 are shown, where endurance data is available.

Other notable examples of developments in the field include flight trials conducted with: the DLR's HyFish [37, 38], an aircraft capable of flight speeds of 200 km/h; Ion Tiger from the US Naval Research Laboratory (NRL) [15]; and Aerovironment's Global Observer prototype Odyssey [15, 49-53].

PEM fuel cells are the most commonly used fuel-cell type in UAS [1]. Their advantages over other fuel-cell chemistries, with respect to mobile applications, include low operating temperatures that permit a short start-up time and relative compactness due to the thinness of their membrane-electrode assemblies. Furthermore, PEM fuel cells can operate with any orientation and do not utilise corrosive fluids [2, 84]. However, the relative expense of the cells and the need for the development of hydrogen infrastructure currently prevent their widespread application [3, 84]. These disadvantages do not advocate the abandonment of PEM fuel-cell technology as a viable power-generation source, rather the need for further research and development.

1.2 Aim

A Hy-Expert Instructor Fuel Cell System, developed by Heliocentris [85], was purchased to enable DSTO personnel to become more familiar with the performance characteristics of PEM fuel cells and to gain insight into their application to UAS. The Hy-Expert system, which is pictured in Figure 3, consists of a PEM hydrogen fuel cell and devices making up the balance of plant (BOP), each of which is discussed in more detail in the following sections. This report describes the experimental characterisation of the Hy-Expert fuel-cell system. Workplace Health and Safety documentation associated with the testing is provided in Appendix A. The findings will be used to further DSTO's knowledge of PEM fuel cells and their implementation in small tactical UAS.

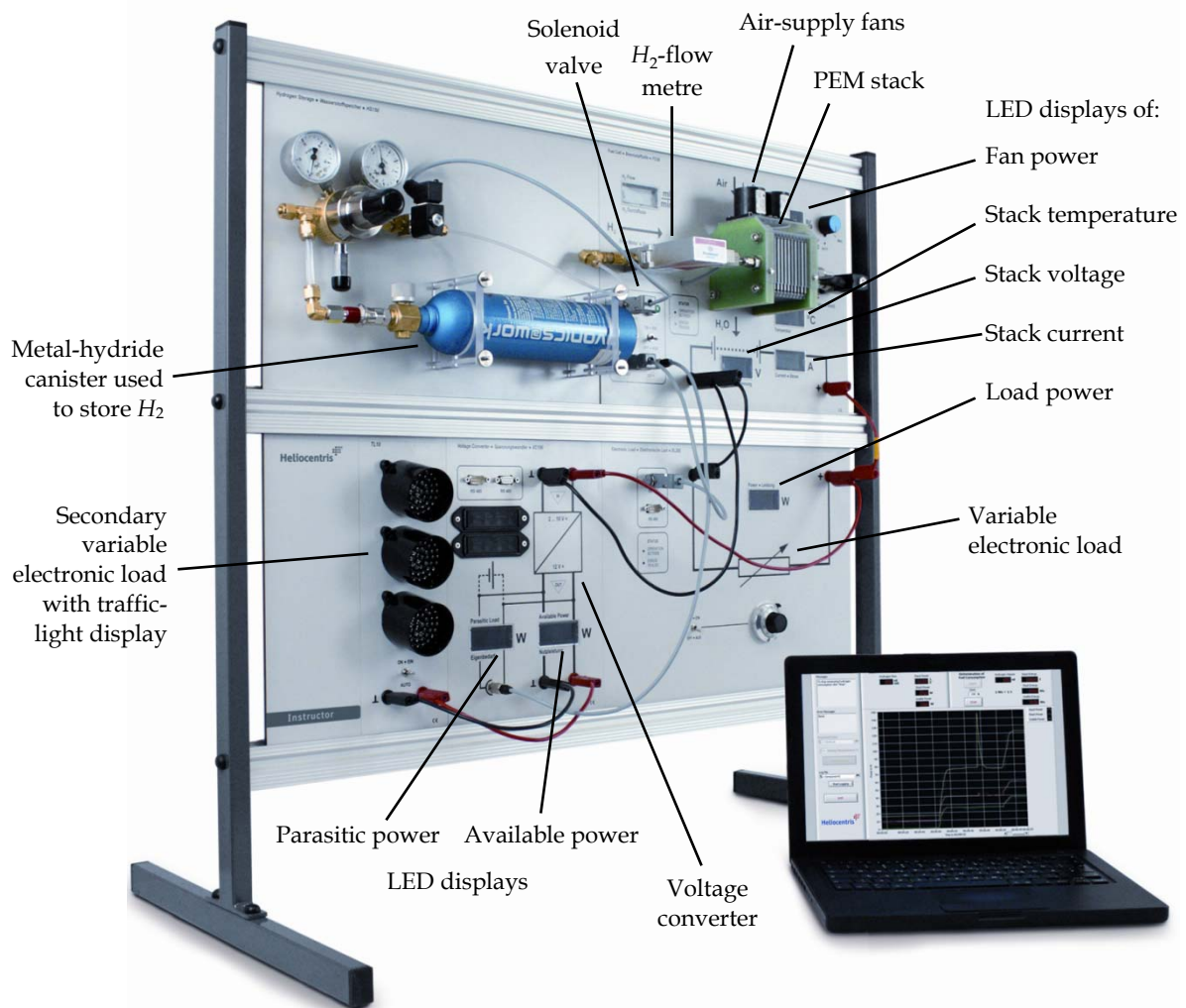


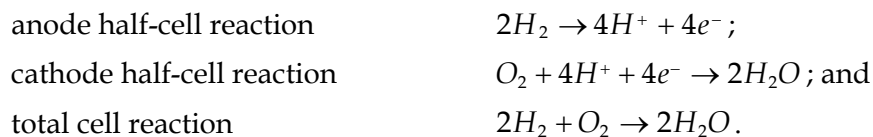
Figure 3 Photograph of the Heliocentris Hy-Expert Instructor Fuel Cell System and a laptop computer that can be used to control its variable load and to record data from the system. Photograph reprinted from [85].

2. Fundamental PEM Fuel-Cell Operation

The basic operation of a PEM hydrogen fuel cell is explained in this section. The driving chemical reaction, basic stack structure, and voltage response are described, as they form the underlying principles upon which the discussions in the following sections are based.

2.1 The Driving Chemical Reaction

A PEM hydrogen fuel cell exploits the reaction between a fuel and oxidant – hydrogen and oxygen, respectively – in the presence of a catalyst (usually platinum) to generate an electric current. Figure 4 depicts a simplified structure of a single cell within a fuel-cell stack. An electrolyte (more specifically a PEM for the Hy-Expert system) is sandwiched between two electrodes, the anode and cathode; and current flows between the electrodes via the load. Hydrogen gas is delivered to the anode, which contains the platinum catalyst, and is decomposed into hydrogen ions and electrons. The mobile electrons generate the current for the load, and the hydrogen ions travel through the PEM to the cathode. Ideally the PEM is a hydrated electrolyte that allows the transmission of ions, but not electrons. Oxygen gas is delivered to the cathode, where, in the presence of the platinum catalyst, it reacts with the hydrogen ions and electrons to produce water. The cell reactions are:



2.2 Physical Structure

The primary components of a fuel-cell stack are the PEM, electrodes, and bipolar plates. A brief description of each component is given below, and a schematic layout of a generic fuel-cell stack is depicted in Figure 5. The reader is also referred to the work of Larminie [2], who provides a perspicuous and detailed discussion of fuel-cell construction.

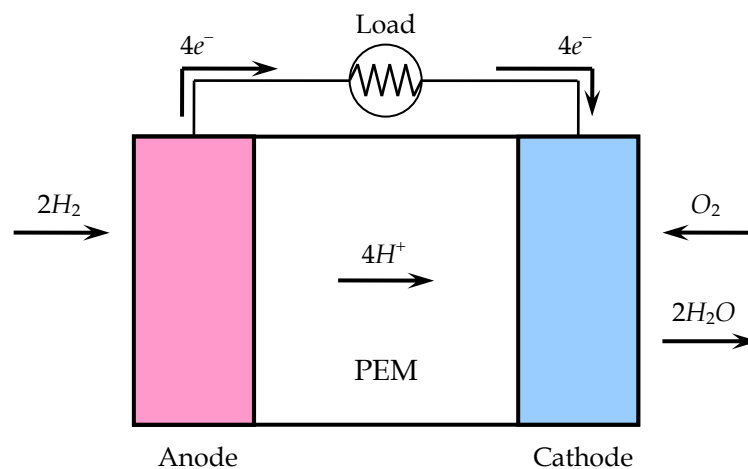


Figure 4 The basic operation of a single PEM hydrogen fuel cell

2.2.1 Polymer-Electrolyte Membrane

The PEM is sandwiched between the two electrodes and ideally permits the flow of hydrogen ions, but not electrons. The membrane is a polymer electrolyte, which at a molecular level consists of hydrophilic regions within a relatively tough and strong hydrophobic structure. The hydrogen ions are therefore able to flow between the hydrated regions, creating what is essentially a dilute acid [2, 3].

2.2.2 Electrodes

Both the anode and cathode generally consist of a carbon-supported catalyst fixed to a conductive material, such as carbon cloth. The carbon cloth provides the mechanical structure for the electrodes and, given its hydrophobic nature, expels product water to the surface where it can evaporate. The carbon cloth also diffuses the gas onto the catalyst; thus, it is often referred to as the gas-diffusion layer (GDL).

2.2.3 Bipolar Plates

The voltage of a single fuel cell is relatively small (ideally about 1.2 V, though usually significantly less). Therefore, to deliver a viable voltage to the load, a number of cells are connected in series to produce a *stack*. The bipolar plate provides a means of interconnecting adjacent cells, collecting current from multiple points on the anode and delivering it to multiple points on the adjacent cathode. If a single-point connection (*i.e.*, a wire) were used to connect adjacent cells, larger voltage losses would result. Channels cut into the bipolar-plate surfaces distribute hydrogen and oxygen to the electrodes.

2.3 Voltage Response

Voltage- and power-current characteristic curves depict the basic behaviour of a fuel cell under load and can be used to size fuel-cell stacks for a given application [86]. Thus, with knowledge of the normal mission profile of a UAS and the resultant demands of the motor

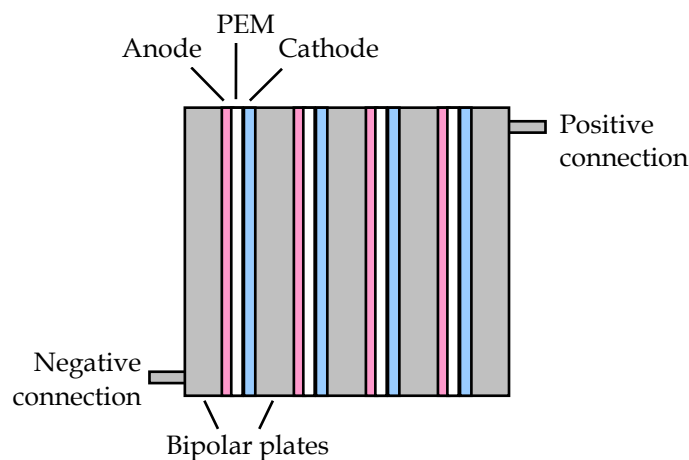


Figure 5 Schematic of a generic PEM fuel-cell stack

and avionics, an appropriate fuel-cell system may be selected. Figure 6 depicts a typical fuel-cell voltage–current characteristic. In an ideal system, the stack output voltage would be independent of load current. However, it is evident from Figure 6 that the stack voltage decreases with increasing load due to irreversibilities in the fuel cell. The dependence of output voltage on load current poses a significant issue for implementing a fuel cell into a UAS, where a portion of the fuel cell’s output would be used to power on-board electrical devices. Such devices generally require a constant voltage; therefore, a voltage regulator would be required to provide a fixed voltage from a fuel cell.

The primary losses inherent in fuel-cell systems include activation over-voltage, fuel crossover and internal currents, Ohmic losses (resistances in the stack and external to it), and concentration losses [2, 3, 87]. An understanding of the mechanisms behind these losses is critical for understanding the factors that affect fuel-cell performance.

2.3.1 Activation Over-Voltage

A high activation over-voltage is the result of a low current-exchange density. Under this condition, a significant portion of the generated voltage is required to drive the chemical reaction in the desired direction. The over-voltage is responsible for the non-linear reduction in voltage at low stack currents (as depicted in Figure 6). Activation over-voltage may be reduced by several means, most of which act to increase the current-exchange density. A higher stack-operating temperature can be used to reduce the magnitude of the activation over-voltage; however, the greater the operating temperature of the stack, the longer the period of time required to start-up the fuel cell [2, 84, 88], which could be undesirable for UAS applications. Furthermore, the increased thermal signature could be detrimental

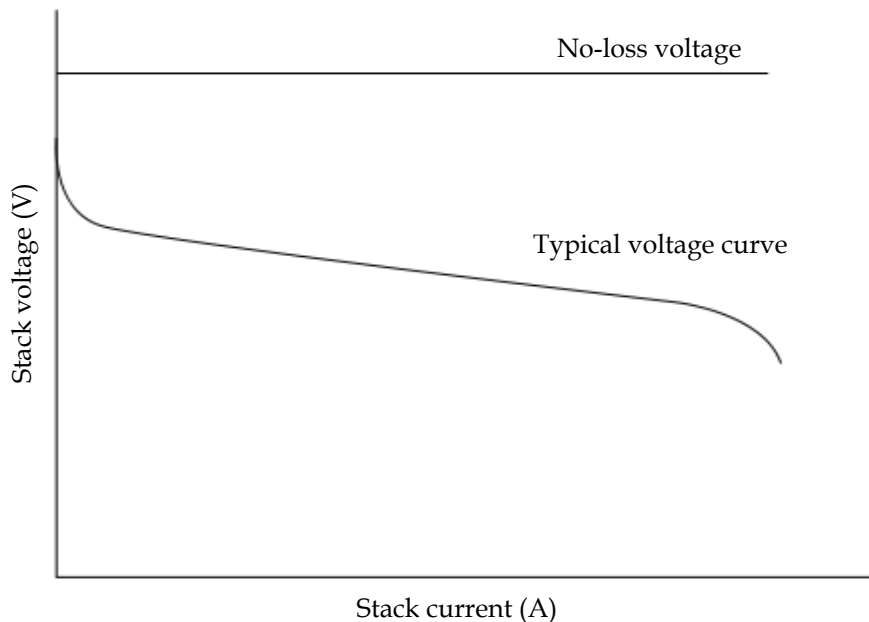


Figure 6 A typical fuel-cell voltage–current curve, where the stack voltage falls below the ideal no-loss voltage with increasing stack current

to mission performance in a military scenario. These issues highlight the compromise that must often be made between power-plant performance and mission effectiveness. Other methods of reducing activation over-voltage include the use of more effective catalysts and increased electrode-surface roughness for increased surface area. A fuel cell with these properties, at the expense of higher cost [84], will possess a greater current-exchange density.

2.3.2 Fuel Crossover and Internal Currents

The PEM allows small quantities of hydrogen gas and electrons to pass through it (a process termed fuel crossover), thus wasting electrons that could have been provided to the load. For low-temperature cells, a noticeable drop in open-circuit voltage is observed. This is depicted in Figure 6, where the open-circuit voltage is less than the no-loss voltage, despite the stack current being zero. As with reducing activation over-voltage, utilising a fuel cell with a higher operating temperature would reduce this loss; however, the consequence would again be a longer start-up time.

2.3.3 Ohmic losses

Ohmic losses are the result of resistances internal to the system and include the resistance to electron flow through the electrodes and connecting circuitry and the resistance to the flow of ions through the electrolyte. The linear decrease in voltage for intermediate current densities seen in Figure 6 is a consequence. Ohmic losses may be reduced in a number of ways, including using highly conductive electrodes and bi-polar plates, minimising the thickness of the PEM, and assembling the stack with greater pressure in order to decrease contact resistances. However, such modifications are likely to increase manufacturing costs. The weight and volume savings due to a reduction in PEM thickness would be beneficial for UAS applications. Such changes may however be impractical as the electrolyte is the material onto which the electrodes are built; thus, a sufficient amount of robustness is necessary [2].

2.3.4 Concentration Losses

Concentration losses result from the mass-transport limitations of the system. At high current densities, the limited rate of supply of reactants and evacuation of products leads to a decrease in concentration of the reactants at the electrodes. Due to the decrease in concentration, the supply of reactants does not meet the demand; and a non-linear reduction in voltage occurs at high current densities, as shown in Figure 6. Given the relatively large dimensions (on the order of millimetres and centimetres) of the reactant-providing flow channels in the bipolar plates of conventional fuel cells, the mass transport is dominated by convection and the laws of fluid dynamics. However, flow in the small pores (on the order of microns) in the GDL is dominated by diffusion. High flow rates in the channels allow good distribution of reactants; however, the rate may be too fast to allow diffusion through the GDL and catalyst layers [89]. To reduce concentration losses, optimisation of the flow within these regions of the fuel cells is required.

3. System Overview

3.1 Specifications of the Hy-Expert Fuel Cell

The specifications of the Hy-Expert fuel-cell stack are provided in Table 1 [85]. As indicated, the Hy-Expert system utilises a 40-W PEM hydrogen fuel-cell stack with supporting BOP devices. Via a control system, the BOP devices administer thermal and water management, the supply of hydrogen and oxygen, and voltage conversion for parasitic loads. Hydrogen is supplied from a metal-hydride storage canister (though other supply options, such as compressed gas cylinders, are available) and fans provide air for the supply of oxygen and for thermal control. An electronic-load module is used to adjust the power drawn from the fuel cell; and various parameters, including power, voltage, current, hydrogen flow rate, and fan power, can be observed on various light-emitting diode (LED) displays (Figure 3). A voltage-converter module provides the required fixed voltage for the parasitic loads; however, the BOP may also be powered via the mains-power grid, as shown in Figure 7 (refer to §6 for details about the Hy-Expert in grid-independent mode).

The Hy-Expert was not designed for use in a UAS. For example, the fuel-cell stack implemented in a 16.4-kg UAS developed at the Georgia Technology Research Institute (GTRI) had a peak output power of 470 W and a mass of 5.0 kg [5]. Clearly, the Hy-Expert produces significantly less power and therefore would not be able to meet the demands of a similarly sized aircraft. However, the Hy-Expert exhibits similar characteristics to larger systems and therefore provides valuable insight into the issues that should be considered when designing fuel-cell-powered aircraft.

3.2 Voltage and Power Response

The initial step in characterising the Hy-Expert system was to determine its voltage and power response under a static load. In the experiments described in this section, voltage- and power-current curves were determined experimentally, and the Ohmic losses of the

Table 1 Hy-Expert stack specifications [86]

Parameter	Specification
Number of cells, $no.cells$	10
Active surface area, A	25 cm ²
Rated power output	40 W
Maximum power output, $P_{stack,max}$	Approximately 50 W
Open-circuit voltage	Approximately 9 V
Current at rated power	8 A
Voltage at rated power	5 V
Maximum current, $I_{stack,max}$	10 A
Hydrogen consumption at rated output	Approximately 580 mL/min (at normal conditions)
Maximum permissible cell temperature	Operation: 50 °C; starting: 45 °C
Mass of stack, m_{stack}	3.5 kg

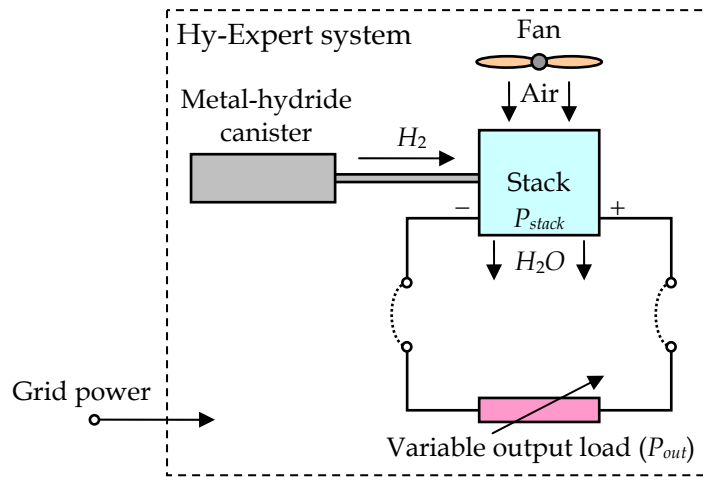


Figure 7 Hy-Expert system in grid-dependent mode, in which the grid powers the BOP devices, including fans, valves, LEDs, etc.

system were quantified. Other properties of the Hy-Expert system were determined, including cell voltage and current density. Based on these values, an example of basic fuel-cell design is given in §7.1. A fuel cell's dynamic response to fluctuating loads is also important, particularly in vehicular applications. Unfortunately, time-resolved measurements could not be acquired using the equipment provided with the Hy-Expert system; therefore, its dynamic behaviour is not documented here. The authors will address the dynamic characteristics of fuel cells in future studies.

3.2.1 Voltage- and Power-Current Characteristic Curves

The Hy-Expert system was characterised at its normal operating temperature of 40 °C. The stack current, I_{stack} , was varied between 0 and 10 A, using the variable output-load module; and the stack voltage, V_{stack} , was measured at various points within this range. From these parameters, the power output by the stack, P_{stack} , was computed by use of:

$$P_{stack} = I_{stack} \cdot V_{stack} \quad (1)$$

The measured voltage-current and power-current curves are depicted in Figures 8(a) and (b), respectively. The voltage-current curve conforms to the expected behaviour of a PEM fuel cell, depicted in Figure 6; and the power-current curve shows that the power increases at a decreasing rate as the stack current increases, due to the reduction in voltage. The maximum power appeared to be ~50 W; however, given that the Hy-Expert system cuts out at 10.5 A – as a protective mechanism against excessive load current – it was not possible to determine this value experimentally.

The voltage of a single cell in the Hy-Expert stack, V_{cell} , is simply the stack voltage divided by the number of cells, $no.cells$; thus,

$$V_{cell} = \frac{V_{stack}}{no.cells} \quad (2)$$

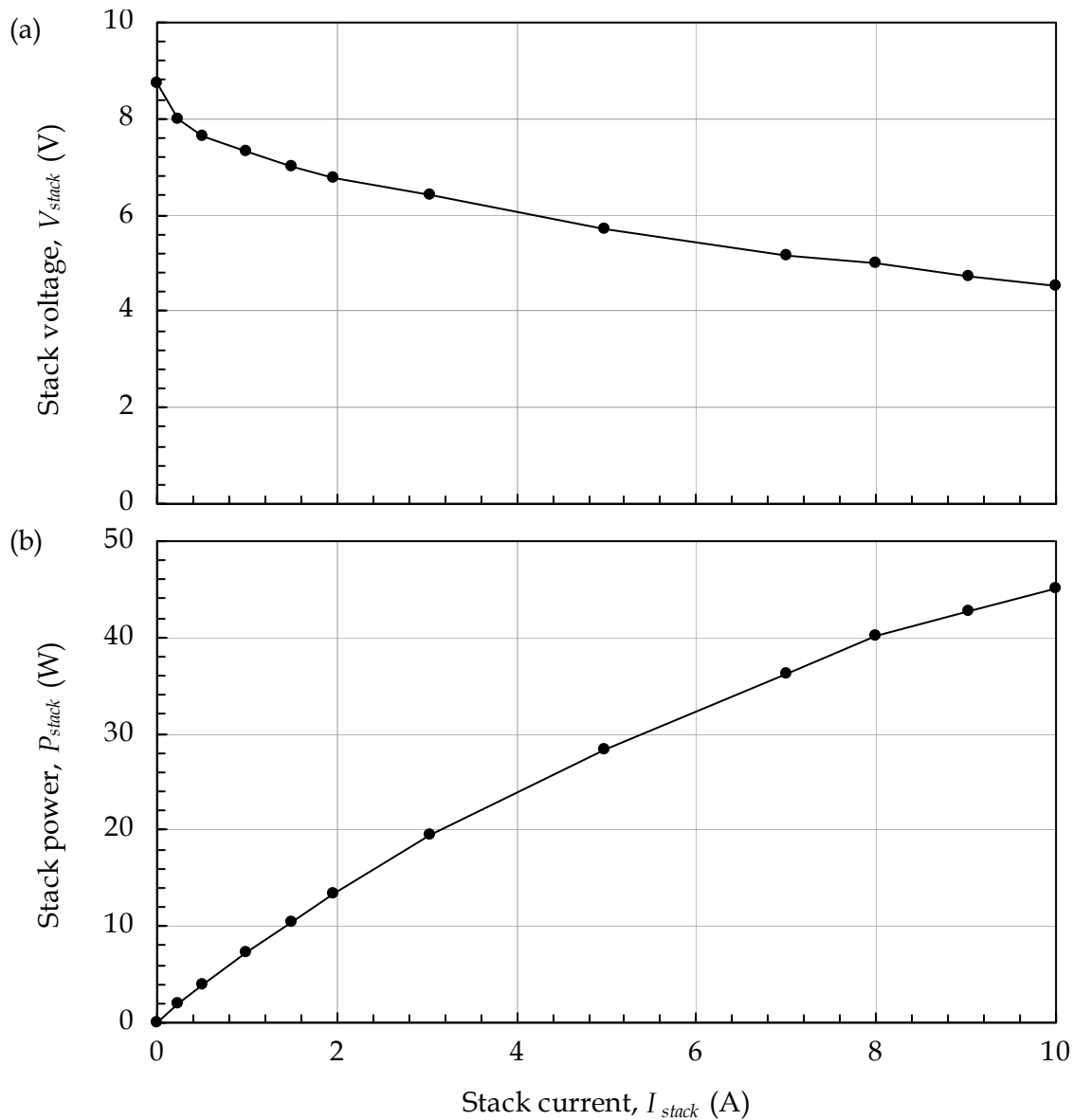


Figure 8 (a) Voltage-current curve and (b) power-current curve for the Hy-Expert stack

As shown in Figure 8(a), at the maximum-current condition ($I_{stack} = I_{stack,max} = 10$ A), the stack voltage is 4.5 V. Given that there are ten cells in the stack, the cell voltage is thus found to be 0.45 V, at the maximum stack-current condition. Note that V_{cell} is significantly less than the ideal no-loss voltage of 1.2 V [2, 84].

Furthermore, the current density, ρ_{cell} , of the stack may be calculated by use of the expression:

$$\rho_{cell} = \frac{I_{stack}}{A}, \quad (3)$$

where A is the active surface area, which for the Hy-Expert stack is 25 cm^2 . At the maximum-current condition, where $I_{stack} = 10 \text{ A}$, the current density is therefore 0.4 A/cm^2 . The specific power of the stack, ρ_p , is defined as the ratio of the maximum power of the stack to its mass; thus,

$$\rho_p = \frac{P_{stack,max}}{m_{stack}}, \quad (4)$$

where m_{stack} is the stack mass (3.5 kg for the Hy-Expert). As the maximum output power is $\sim 50 \text{ W}$, Equation (4) indicates that the specific power of the Hy-Expert stack is 14 W/kg .

An understanding of the relative merit of the Hy-Expert stack (or system) as a possible source of power on-board an aircraft may be gained by comparing its properties with those of systems trialled on UAS. For example, the fuel-cell-powered UAS developed and successfully flown by GTRI [5] employed a stack with a significantly higher specific power than the Hy-Expert stack: 94 W/kg compared with 14 W/kg for the Hy-Expert stack. Given that the performance of an aircraft is largely restricted by its power-to-weight ratio [90], the Hy-Expert system, as previously mentioned, is far from ideal for such an application. A number of methods could however be used to improve the specific power of the fuel cell, including:

- improving the catalyst to increase the current density and, with it, the power density;
- using thinner electrodes, PEMs, and bi-polar plates, thus reducing the volume and mass of the stack for the same power output; and
- minimising inactive surfaces to reduce the volume and mass of the stack while maintaining its power output.

3.2.2 Determination of Ohmic Losses

The Hy-Expert stack operates predominantly in the linear region of the voltage-current characteristic curve. In this region, Ohmic losses dominate the voltage response of the system. The equivalent circuit for the fuel-cell system, depicted in Figure 9, aids in understanding the resistance losses present in the system. In Figure 9, the stack voltage (V_{stack} , as before) and the output terminal voltage, V_{term} , which is the voltage across the variable output load, are labelled; and V_o represents the current source, in this case, the fuel-cell stack. The internal resistances within the stack, R_{stack} , are represented in series with the resistances external to it, R_{addl} , which includes the cables connecting the stack to the load.

To quantify the effect of Ohmic losses on the fuel cell's output, the voltage-current curve was measured for a second time; however, in this case, both the stack voltage and the output terminal voltage were recorded. Typical voltage-current characteristic curves were observed for each, as shown in Figure 10. The recorded stack voltage was slightly different to that shown in Figure 8(a) due to differences in the conditioning of the fuel cell prior to the measurements (*e.g.*, a difference in stack temperature). The terminal voltage displayed a steeper decline with increasing stack current in the linear region than did the stack voltage due to the resistance within the cables that connect the stack to the output terminals.

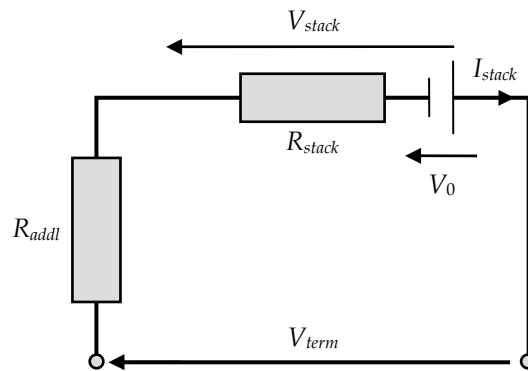


Figure 9 Equivalent circuit representing internal resistances in the Hy-Expert system

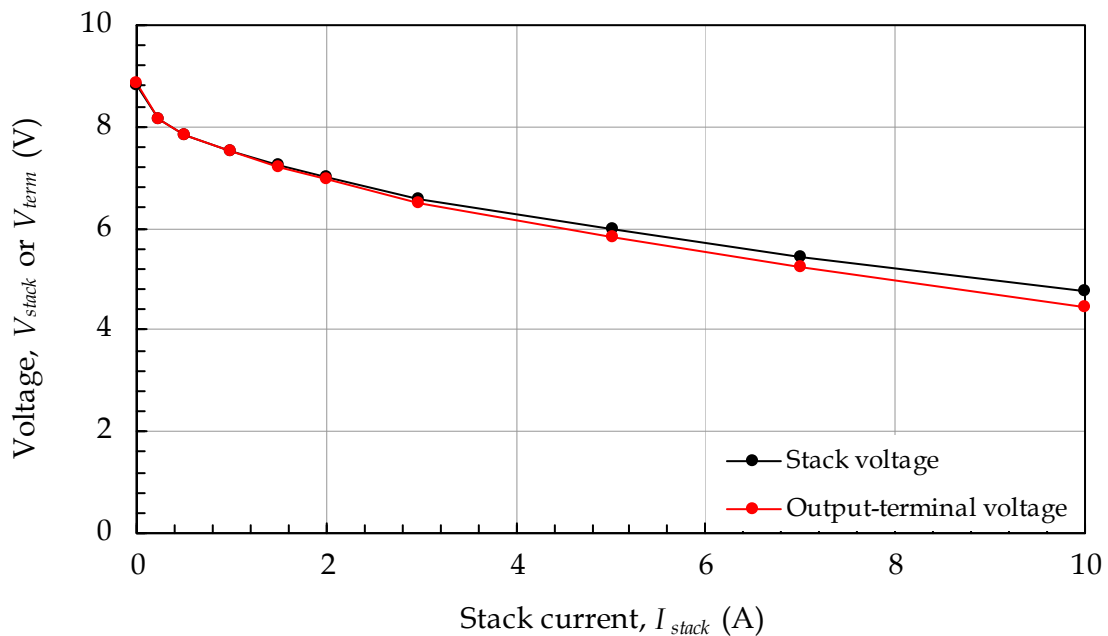


Figure 10 Voltage–current characteristic curves, measured across the stack (V_{stack}) and at the output terminals (V_{term})

The internal resistance of the stack was determined from the slope of the linear region of the stack voltage–current curve shown in Figure 10. By applying the expression:

$$R_{stack} = -\frac{\Delta V_{stack}}{\Delta I_{stack}} \quad (5)$$

over a portion of the linear region, the stack resistance was found to be 0.26Ω . The maximum power lost within the stack, $P_{stack,loss}$, was then determined from the maximum operating current ($I_{stack,max} = 10 \text{ A}$) and the stack resistance, by use of:

$$P_{stack,loss} = I_{stack,max}^2 R_{stack} \quad (6)$$

The maximum stack power loss was found to be 26 W.

The total internal resistance of the system, R_{tot} , was determined from the slope of the linear region of the output-terminal voltage–current curve shown in Figure 10, by use of an expression analogous to Equation (5):

$$R_{tot} = -\frac{\Delta V_{term}}{\Delta I_{stack}}. \quad (7)$$

The resistance external to the stack was found to be 0.03Ω , the difference of the total system internal resistance and the stack resistance. The voltage drop due to the additional resistance is given by $I_{stack} R_{addl}$, which yields a value of 3 V at the maximum operating current of 10 A, in agreement with the maximum difference between the stack and output-terminal voltages observed in Figure 10. The power loss external to the stack, $P_{ext,loss}$, was calculated to be 3 W at 10 A, by use of the expression:

$$P_{ext,loss} = I_{stack}^2 R_{addl}. \quad (8)$$

As expected, the losses within the stack were significantly greater than the losses internal to the system, but external to the stack. This result highlights the significance of internal Ohmic losses on the performance of a fuel-cell system.

4. System Efficiencies

Along with the fuel-cell mass, volume, and cost, fuel efficiency may be important in UAS applications, if long endurance is desired and the capacity for on-board fuel storage is limited. As described here, the stack power (fuel) efficiency of the Hy-Expert system was characterised across a range of loads; and the optimum operating point with respect to stack efficiency was identified. Consideration was given to factors that influence stack efficiency, including the voltage and current efficiencies of the fuel cell. The impact that optimising stack efficiency would have in UAS applications is discussed in this section.

4.1 Stack Efficiency

When the voltage-current characteristic curve for the Hy-Expert stack was measured (§3.2.1), the volumetric flow rate of hydrogen, \dot{V}_{H_2} , was also recorded. The data, shown in Figure 11, can be used to determine the stack power efficiency, η_{stack} , which is defined as the ratio of the power output by the stack (P_{stack} , as before) to that provided in the form of hydrogen gas, P_{in} . The rate at which energy enters the system may be expressed as:

$$P_{in} = LHV \cdot \dot{V}_{H_2}, \quad (9)$$

where LHV is the lower heating value (LHV) of hydrogen, which at standard conditions (25 °C and 100 kPa) is 10.8 MJ/m³ [86]. (Other, slightly different measures of the energy density of hydrogen gas are described in §4.3.) Thus, the stack efficiency can be written as:

$$\eta_{stack} = \frac{P_{stack}}{P_{in}} = \frac{V_{stack} I_{stack}}{LHV \cdot \dot{V}_{H_2}}. \quad (10)$$

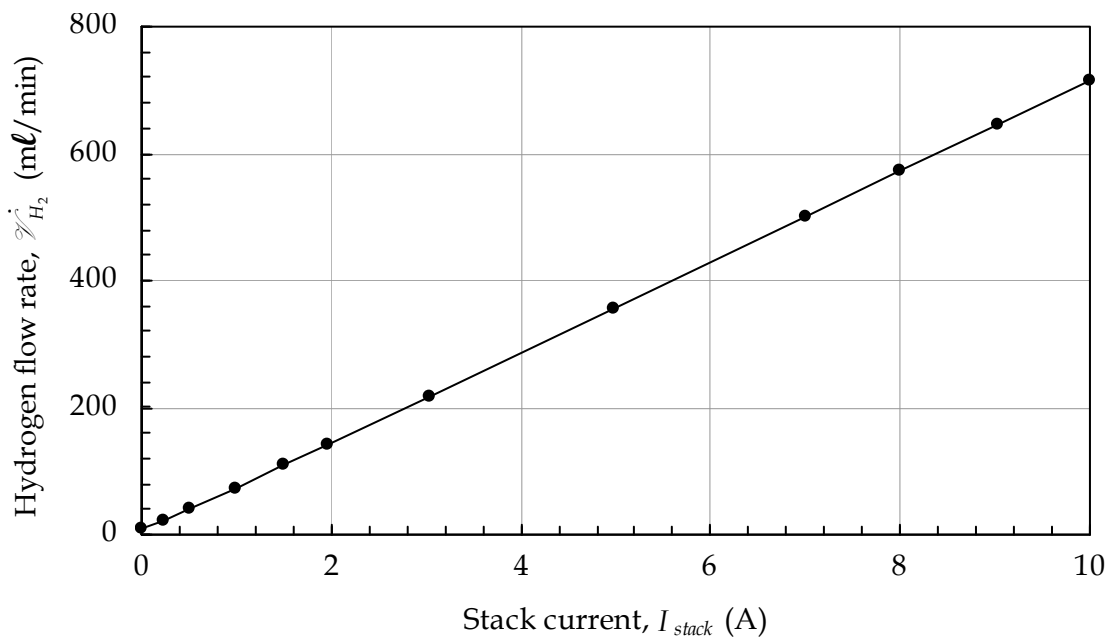


Figure 11 Hydrogen flow rate as a function of stack current for the Hy-Expert system

The computed stack efficiency is plotted in Figure 12, along with the stack power. The optimum efficiency of the Hy-Expert's fuel-cell stack (~55%) occurs in the low-load range (at ~1 A), whereas the delivered power increases monotonically with stack current. This is typical of PEM fuel cells [2]. When selecting a fuel cell for a given application, a decision must be made to optimise fuel efficiency or output power. To optimise efficiency, a fuel cell with a greater maximum power than is used under normal conditions is required; thus, the fuel cell will be larger and more expensive than it otherwise would be. Although this is reasonable for stationary applications, it is not appropriate for most UAS applications, which have stringent weight and internal-space (volume) limitations. Thus, UAS designers generally maximise output power, at the expense of fuel efficiency, to achieve reductions in the weight, volume, and cost of the fuel cell.

4.2 Voltage and Current Efficiencies

The stack power efficiency can be decomposed into a voltage efficiency, η_V , and a current efficiency, η_I , and expressed as:

$$\eta_{stack} = \eta_V \cdot \eta_I. \quad (11)$$

The voltage efficiency indicates the quality of conversion of the internal energy of the participating molecules in the fuel-cell reaction into electricity [86] and is given by:

$$\eta_V = \frac{V_{stack}}{no.cells \cdot V_{rev,LHV}}, \quad (12)$$

where $V_{rev,LHV}$ is the reversible thermodynamic voltage at the LHV, which is defined as

$$V_{rev,LHV} = \frac{LHV}{\mathcal{F} \cdot z_{H_2}}. \quad (13)$$

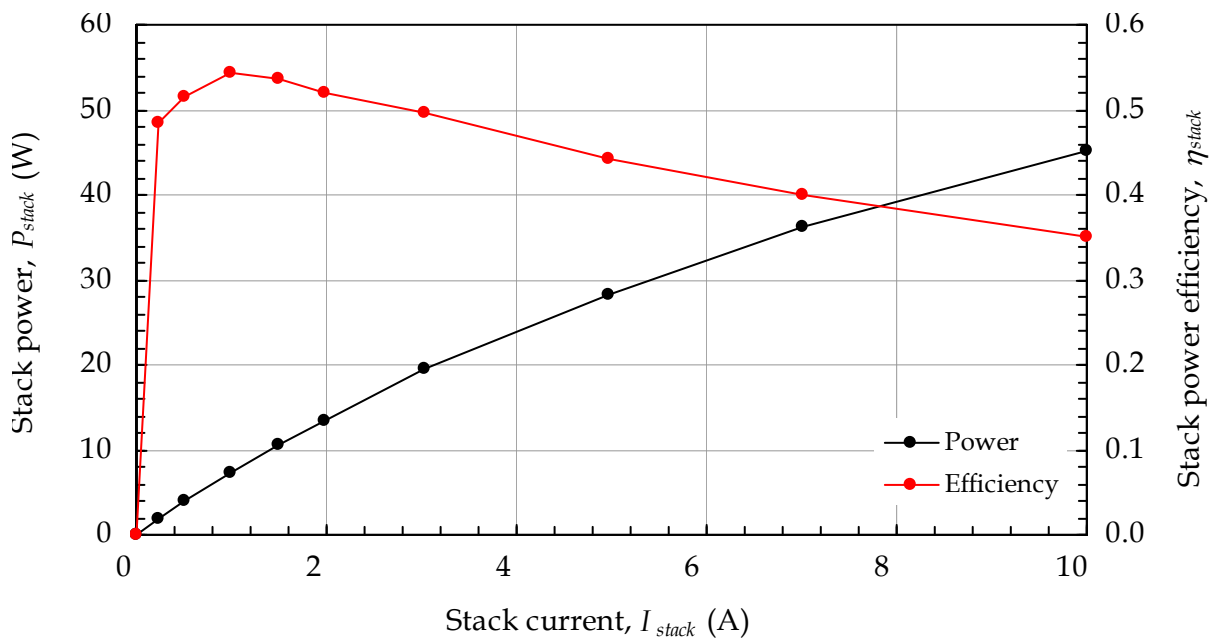


Figure 12 Stack efficiency and power as functions of stack current for the Hy-Expert system

Here, \mathcal{F} is Faraday's constant (9.648×10^4 C/g-mol) and z_{H_2} is the valency of the reaction for hydrogen, $2 e^-$ /ion, as shown in the anode half-cell reactions in §2.1. Equation (13) yields a value of 1.25 V [86]. Ideally, the stack voltage is independent of the load current; however, irreversibilities in the system, as previously described, cause the stack voltage and thus the voltage efficiency to vary with the load current.

The voltage efficiency was calculated as a function of stack current for the Hy-Expert system by use of Equation (12), and the results are depicted in Figure 13. The stack voltage-current curve shown in Figure 8(a) was used; and the number of cells was taken to be ten, the number for the Hy-Expert stack. It should be noted that a voltage efficiency of unity cannot be achieved, even if all the losses that affect the voltage characteristic are neglected. This is because the reaction product (water) is assumed to be at the same temperature as the reactants. However, as the fuel-cell membrane has a higher temperature than the ambient, the water is delivered at a higher temperature than the supplied reactants. Thus some energy is lost as heat in the water. If these losses were included in the reference voltage, its value would be reduced and the voltage efficiency would be higher. Nonetheless, Figure 13 illustrates the trend of voltage efficiency with stack current.

The current efficiency is defined as the ratio of the stack current (I_{stack}) to the maximum current theoretically possible given the rate of fuel consumption in the system, I_{th} . The latter quantity may be determined from Faraday's laws of electrolysis, and expressed as:

$$I_{th} = \frac{\dot{\mathcal{V}}_{H_2} \cdot \mathcal{F} \cdot z_{H_2}}{no.cells \cdot \mathcal{V}_m}, \quad (14)$$

where \mathcal{V}_m is the molecular standard volume (22.4 l/g-mol at standard conditions), which

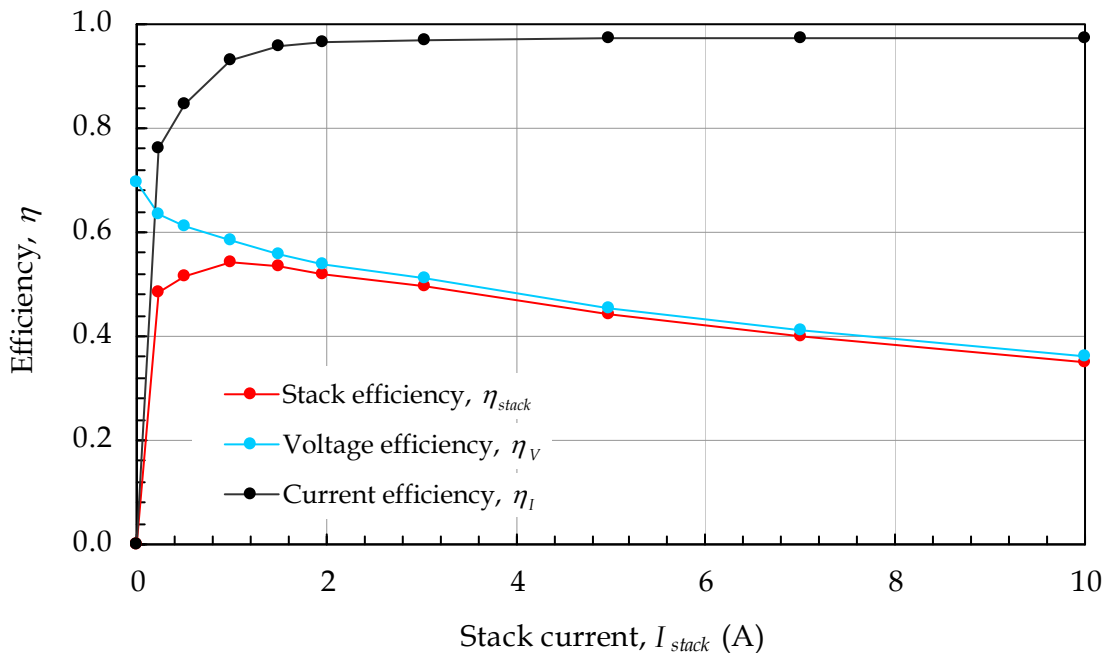


Figure 13 Voltage, current, and stack efficiencies of the Hy-Expert fuel cell

can be used to convert a volumetric quantity of a gas into a number of gram-moles, if the gas is assumed to be ideal. The current efficiency is thus given by:

$$\eta_I = \frac{I_{stack}}{I_{th}} = \frac{I_{stack} \cdot no.cells \cdot \mathcal{V}_m}{\mathcal{V}_{H_2} \cdot \mathcal{F} \cdot z_{H_2}} \quad (15)$$

The current efficiency for the Hy-Expert stack is shown in Figure 13. Losses of hydrogen gas, through leakages, chemical side reactions, and fuel crossover, result in reductions in the current efficiency. As the load current increases, however, these losses become less significant; and, as shown in Figure 13, the current efficiency asymptotically approaches a value close to unity (0.972). The current efficiency in this case does not reach unity, however; and the reason for this is not entirely clear. Some potential causes are discussed in §5.1.1.

4.3 Alternative Methods of Calculating Efficiency

Several different reference voltages may be used to calculate fuel-cell efficiency. These include the LHV, the higher heating value (HHV), and Gibbs free energy, defined below.

LHV: Is the amount of energy released in a reaction, where it is assumed that the pre-reaction temperature is 25 °C and the post-reaction temperature is an arbitrary 150 °C. Therefore, it assumes the product water is in a vaporous state and thus neglects the enthalpy of condensation. The LHV was used to determine the stack efficiency of the Hy-Expert system, as the majority of its product water is in a vaporous state. The reversible thermodynamic voltage for the LHV is $V_{rev,LHV} = 1.25$ V, as indicated by Equation (13).

HHV: Is the amount of energy released in a reaction in which it is assumed that the pre- and post-reaction temperatures are 25 °C. If the HHV is used, it is assumed that the product water is in a liquid state; thus, the enthalpy of condensation is included. The reversible thermodynamic voltage for the HHV is defined as $V_{rev,HHV} = HHV / (\mathcal{F} \cdot z_{H_2}) = 1.48$ V, where $HHV = 12.8$ MJ/m³ for hydrogen at standard conditions.

Gibbs free energy: Is the reaction enthalpy minus the reaction entropy ($\Delta g_f = 10.6$ MJ/m³ for hydrogen at standard conditions). It therefore describes the maximum amount of energy that can be extracted from the system. The reversible thermodynamic voltage related to the free-reaction enthalpy is $V_{rev}^0 = \Delta g_f / (\mathcal{F} \cdot z_{H_2}) = 1.23$ V.

Therefore, depending on the choice of reference voltage, different efficiency values will be calculated. For example, at a stack voltage of 8.74 V (the open-circuit voltage for the Hy-Expert stack), the voltage efficiencies relating to LHV, HHV, and Gibbs free energy are 0.70, 0.59, and 0.71, respectively. The basis on which the voltage and stack efficiency are computed should thus be taken into account when comparing different fuel-cell systems.

5. Reactant Supply and Thermal Management

5.1 Hydrogen Supply

For any fuel cell, the current demanded by the load governs the quantity of hydrogen consumed within the stack (up to a point), as illustrated by the discussion in §4.1. Thus, by estimating the power demands of a given UAS mission, the required storage capacity may be determined. As described in this section, the measured relationship between load current and hydrogen flow rate for the Hy-Expert system was compared with a theoretical relationship; and the quantity of escaping hydrogen gas was estimated. The advantages and disadvantages of various methods of hydrogen storage were also considered.

5.1.1 Hydrogen Flow Rate *vs.* Load Current

As shown in Figure 11, the flow rate of hydrogen into the fuel-cell system increases linearly with stack current at a rate of $\Delta \dot{\mathcal{V}}_{H_2} / \Delta I_{stack} = 71.1 \text{ mL/min/A}$. This is consistent with Faraday's first law, Equation (14), which indicates that the amount of fuel consumed at the electrode is proportional to the quantity of electricity transferred. However, the hydrogen flow rate was non-zero (8 mL/min) at no-load operation. Given that the load current was zero, it is unlikely that a chemical reaction was taking place at the anode. Instead, the non-zero flow rate was attributable to hydrogen leaking from the system. The leakage of small quantities of hydrogen occurs through imperfect connections and is normal for hydrogen-fuelled systems. For this reason, it is usually recommended that a ventilation system be used when operating a fuel cell indoors and that the concentration of hydrogen gas in the surrounding environment be monitored.

The theoretically expected ratio of hydrogen flow rate to stack current may be determined by rearranging Equation (14) to obtain:

$$\frac{\dot{\mathcal{V}}_{H_2}}{I_{th}} = \frac{\mathcal{V}_m \cdot no.cells}{\mathcal{F} \cdot z_{H_2}}. \quad (16)$$

This quantity may be thought of as the ratio of the actual (measured) hydrogen flow rate, $\dot{\mathcal{V}}_{H_2,act}$, to the stack current that is expected to be produced when the hydrogen is reacted, I_{th} . Alternatively, it may be considered the ratio of the flow rate theoretically needed to produce a given stack current, $\dot{\mathcal{V}}_{H_2,th}$, divided by the stack current, I_{stack} . Thus,

$$\frac{\dot{\mathcal{V}}_{H_2,act}}{I_{th}} = \frac{\dot{\mathcal{V}}_{H_2,th}}{I_{stack}} = \left[\frac{\dot{\mathcal{V}}_{H_2}}{I_{stack}} \right]_{th}. \quad (17)$$

Furthermore, if a constant leakage rate is present in the system, Equations (16) and (17) may be used to determine the increase in hydrogen flow rate theoretically required for a given increase in stack current, $\Delta \dot{\mathcal{V}}_{H_2} / \Delta I_{stack}$, for an otherwise lossless system:

$$\left[\frac{\dot{\mathcal{V}}_{H_2}}{I_{stack}} \right]_{th} = \left[\frac{\Delta \dot{\mathcal{V}}_{H_2}}{\Delta I_{stack}} \right]_{th} = \frac{\mathcal{V}_m \cdot no.cells}{\mathcal{F} \cdot z_{H_2}}. \quad (18)$$

This yields 69.5 mL/min/A for a ten-cell stack, such as the Hy-Expert stack, or 6.95 mL/min/A/cell.

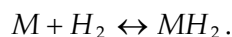
A number of factors could be responsible for the small discrepancy between the theoretical and experimentally obtained values of $\Delta \dot{V}_{H_2} / \Delta I_{stack}$, 69.5 and 71.1 mL/min/A, respectively. These include a small increase in fuel crossover, internal currents and fuel leakage with hydrogen flow rate, or measurement error.

5.1.2 Hydrogen Storage

Storing hydrogen as a compressed gas is a common method on-board UAVs and has been used in a number of successful flight demonstrations [1]. The popularity of this technology is largely due to its relative simplicity of implementation. However, a number of disadvantages associated with it have led to the development of alternative storage techniques. Although hydrogen has a high specific energy (energy per unit mass), it has a relatively low energy density (energy per unit volume) at standard conditions, compared with liquid fuels, for example; thus, a high pressure is required to store a large amount of hydrogen in a small space [2]. Furthermore, care must be taken when selecting the canister-casing material, as hydrogen is a very small molecule, capable of diffusing into materials that are impermeable to other gases [2].

The use of cryogenic hydrogen permits a relatively large amount of hydrogen to be stored in a small space. The drawbacks, however, include the energy intensiveness of creating the low-temperature, high-pressure environment required for liquefaction, the dangers of cryogenic substances, and the need for adequate canister insulation, which is likely to add weight and to occupy more space within the aircraft. Nevertheless, in 2005, AeroVironment successfully implemented cryogenic hydrogen storage on-board their Global Observer platform, a first for an aircraft [91]. Although the Global Observer is not a small tactical UAV, instead being intended for high-altitude, long-endurance missions and having a wingspan of 16.4 m, the success of the flight trials demonstrated the potential for using cryogenic hydrogen in aircraft. At the time of the writing this report, however, the authors were not aware of the use of cryogenic hydrogen storage in a smaller UAS.

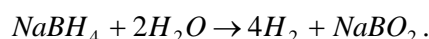
The Hy-Expert system utilises hydrogen storage in a canister containing a metal hydride. The metal alloy effectively absorbs and emits hydrogen gas via the reversible reaction:



The canister is charged by connecting it to a pressurised hydrogen cylinder and can be discharged at near-ambient temperature by opening the canister. The advantage of this system is its energy density, which is significantly improved over that of pure hydrogen (*i.e.*, metal hydride holds more hydrogen per unit volume than hydrogen gas at standard conditions); thus, the storage method is well suited to the limited space on-board a UAS. In addition, the hydrogen is not stored at high pressure; therefore, it does not rapidly discharge if the canister is damaged or unintentionally opened. One of the primary disadvantages of this form of storage, however, is its relatively low specific energy. This is particularly relevant for UAS applications, which have stringent weight restrictions. Further-

more, the system is susceptible to damage from impurities (thus high-purity hydrogen is required to fill the canister) and charging the canister takes a significant period of time (about 1 h for a 5-kg canister [2]).

Hydrogen is not a common battlefield fuel, and other methods of supplying hydrogen in fielded applications have been developed to avoid the need to provide hydrogen gas on the battlefield. Thus, a number of chemical storage techniques are available in which hydrogen gas is released from a compound by a controlled reaction. The use of sodium borohydride, for example, is a particularly successful method that has been implemented in a number of UAS platforms [1]. Hydrogen is released from a sodium-borohydride solution by the following exothermic reaction and supplied to the fuel cell:



The sodium-borohydride solution is quite stable, requiring a catalyst to initialise the reaction. As a result, the reaction is highly controllable. The solution is brought in contact with the catalyst to produce hydrogen, and removal of the catalyst stops the reaction. Sodium borohydride is safe to transport, which is a significant advantage, and it has a desirable specific energy and energy density in comparison to compressed hydrogen. The most significant disadvantage of this technology, however, is its relatively high cost of production, which currently makes the technology impractical for widespread use.

5.2 Air Supply

The supply of air to the Hy-Expert system serves two purposes: it provides oxygen for the fuel-cell reaction and it serves to regulate the stack temperature through convective cooling. To investigate the impact of air supply on fuel-cell performance, the voltage and power response of the Hy-Expert system under normal operation was compared with that when the air supply was significantly reduced. The minimum theoretical airflow rate required to sustain a given load was also determined; and various alternative means of supplying oxygen and regulating fuel-cell temperature were considered. The results are discussed in this subsection.

5.2.1 Fuel-Cell Performance with Restricted Airflow

The voltage- and power-current curves were determined experimentally for two situations. In the first case, the fan was set to AUTO. Thus, the Hy-Expert control system provided sufficient airflow for good fuel-cell performance. In the second case, the fan was fixed at 6% of its full capacity for all loads. The resulting voltage-current curves are depicted in Figure 14. In the low current range (0–2 A), catalytic processes (*i.e.*, activation over-voltage effects) dominate the system's behaviour. Both measured stack-voltage levels decrease with a similar exponential trend, indicating that the 6%-airflow fan setting is sufficient for normal operation at these current levels. At mid-range loads (2–7 A), the system's internal resistances dominate the electronic behaviour of the fuel cell. A slight divergence of the reduced-air characteristic occurs due to the varying conditions of the membrane. The stack temperature increases as a result of the reduced airflow; and membrane drying occurs, which leads to a lower ionic conductivity and a larger voltage drop [86]. At

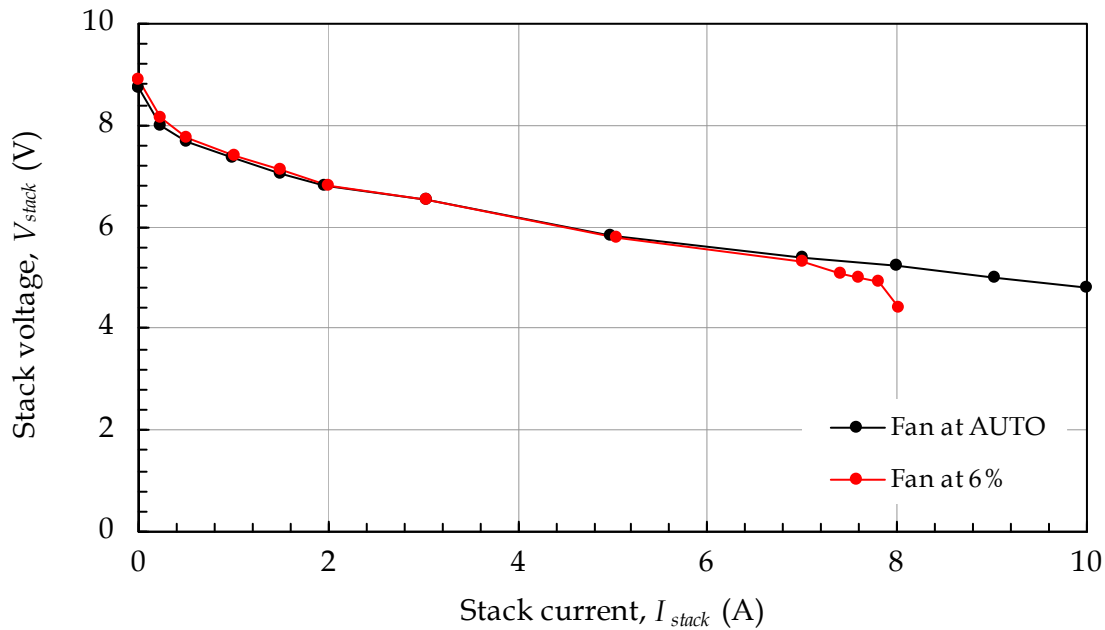


Figure 14 Hy-Expert voltage response under normal and reduced-airflow conditions

high loads (7–10 A), the 6% fan setting provides insufficient air (and therefore insufficient oxygen) to sustain the reaction rate necessary to meet the increased load. As a result, the stack power is reduced; and, given that the load current is fixed, the stack voltage decreases also.

The corresponding power–current curves are shown in Figure 15. A slight divergence between the curves occurs with increasing load; and as discussed previously, the fuel-cell output power drops suddenly in the high-load range when insufficient airflow is supplied.

5.2.2 Required Airflow Rate

As was done in §5.1.1 for hydrogen, the airflow rate theoretically required to meet the demands of a given load (a desired value of I_{th}) can be estimated by use of an expression analogous to Equation (16):

$$\dot{\mathcal{V}}_{O_2} = \frac{I_{th} \cdot \mathcal{V}_m \cdot \text{no. cells}}{\mathcal{F} \cdot z_{O_2}} \quad (19)$$

The valency of oxygen, z_{O_2} , is $4e^-/\text{ion}$, given that for each oxygen molecule, four electrons are transferred in the reaction (see the cathode half-cell reaction in §2.1). Oxygen comprises ~20% of the molecules in atmospheric air; and the required flow rate of air is likewise proportional to the required flow rate of oxygen:

$$\frac{\dot{\mathcal{V}}_{O_2}}{\dot{\mathcal{V}}_{air}} = \frac{\dot{\mathcal{V}}_{O_2}}{\dot{\mathcal{V}}_{air}} = 0.2 \quad (20)$$

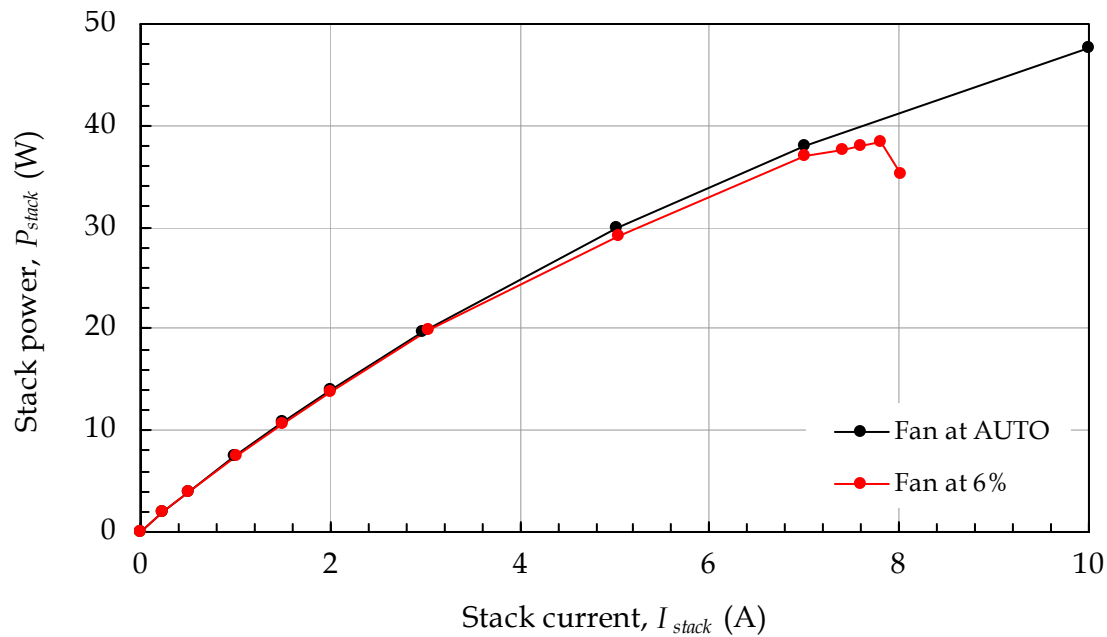


Figure 15 Hy-Expert power response under normal and reduced-air conditions

It should also be noted that fuel cells are generally provided with excess air, quantified as a multiple, λ , of the amount of air required for the reaction. A value of $\lambda = 10$ indicates that ten times more air is supplied than is necessary for the reaction. The airflow needed for cooling is much greater than that needed for the reaction. Therefore, excess air is especially important in systems such as the Hy-Expert system, where airflow serves to control the temperature of the stack as well as to provide oxygen for the reaction. Furthermore, the theoretically computed airflow rate is generally insufficient in practice due to concentration losses about the cathode and other non-idealities. Below a certain concentration, oxygen cannot reach the membrane; thus, the reaction is restrained.

Another issue to consider for UAS is the reduction in air pressure with altitude, which may result in a reduction in oxygen available to the fuel cell. Depending on the altitude at which the UAS will fly and the period of time spent at this altitude, the reduction could be quite significant. For example, at an altitude of 1000 m, the partial pressure of oxygen is approximately 89% of that at sea level [92]. It should be noted that oxygen will still comprise about 20% of the air at this altitude. However, there are fewer air molecules due to the reduction in pressure (*i.e.*, \mathcal{V}_m has a higher value than at standard conditions).

5.2.3 Supply of Oxygen

There are a number of options for providing oxygen to a fuel-cell stack on-board a UAV:

1. atmospheric air may be delivered by a fan or compressor unit for oxygen supply, as well as thermal management;
2. oxygen may be delivered from an on-board storage canister or generator for the fuel-cell reaction, with a separate temperature-management system employed; and

3. natural ventilation resulting from the aircraft's airspeed may be used to provide oxygen for the reaction, as well as thermal management.

Of the options available, the first (used in the Hy-Expert system) appears to be the most desirable. While the second option offers improved fuel-cell performance, due to the use of pure oxygen, the additional apparatus required to store the oxygen would occupy valuable space and add weight to the UAV. Furthermore, the lack of control over natural ventilation in the third option is undesirable. The airflow must be adjustable to meet the oxygen supply demands and to maintain a desirable stack temperature.

5.3 Thermal Management

The stack temperature has a significant effect on the performance of a fuel cell. Therefore, an understanding of how a fuel cell functions across a range of temperatures is necessary in order to optimise its performance across the expected load range. In this section, the voltage response of the Hy-Expert is characterised at two different operating temperatures: a temperature greater than its normal operating temperature of 40 °C and another below. In addition, alternative means of temperature regulation are described.

5.3.1 Effect of Operating Temperature

The response of the Hy-Expert was measured at an initial nominal temperature of 44 °C and at a lower initial temperature of 28 °C. It should be noted that these were the initial temperatures of the stack only; and as the load increased, the stack temperature increased. The results of the experiment are depicted in Figure 16. The curve obtained at the higher temperature is observed to flatten at a lower current than the lower-temperature curve. Therefore, for the same load current, a higher voltage is achieved with an initial temperature of 44 °C than is achieved at 28 °C. This is due to the accelerated rate of reaction resulting from the higher stack temperature. At higher currents, however, the two curves converge. The reduction in voltage of the higher-temperature curve is attributed to the reduction in water content (and therefore conductivity) of the membrane, caused by the further increase in temperature. Furthermore, the increase in temperature increases the resistance of the bi-polar plates, which also has the effect of reducing stack voltage.

5.3.2 Alternative Methods for Thermal Management

Fan-forced airflow systems that provide oxygen and act to cool a fuel-cell stack, such as the one used in the Hy-Expert, benefit from their relative simplicity and can control the temperature of stacks rated to ~100 W reasonably well [2]. However, they may not be suitable for higher-powered stacks, such as those used in UAS, as the high airflow rate required to cool the stack can de-humidify the PEM. A number of methods exist for overcoming this problem. One method involves the use of separate reactant air and cooling air streams, such that the cooling air does not come in contact with the electrodes and thus does not dry out the PEM. A moisturiser can also be used to humidify the air and/or hydrogen entering the fuel-cell stack, thus preventing excessive drying of the PEM and effectively increasing the maximum operating temperature of the stack. Alternatively, a

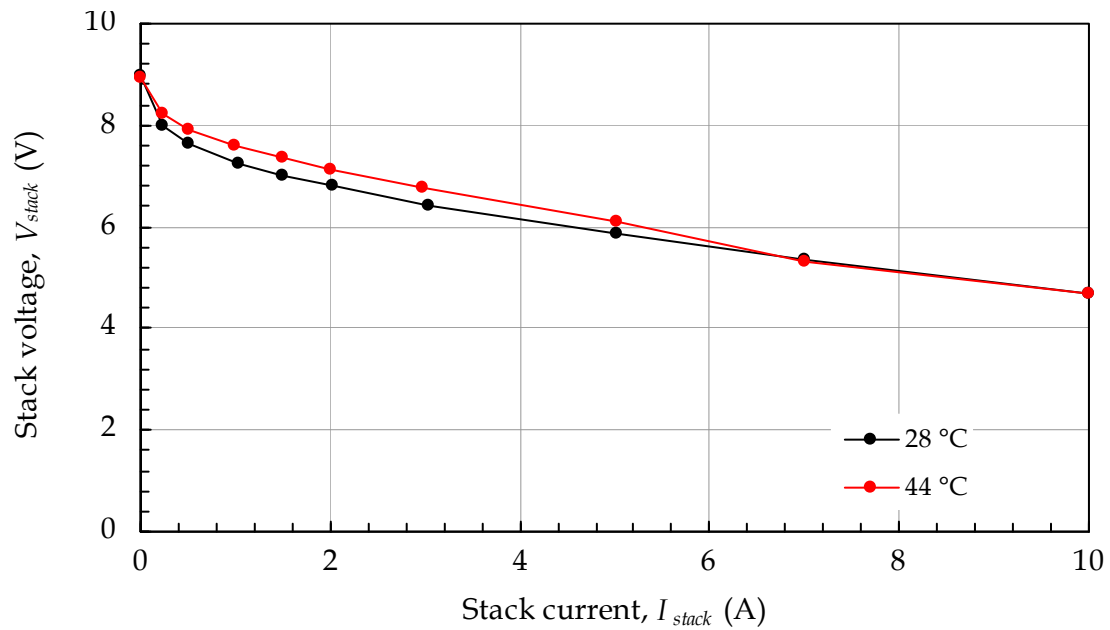


Figure 16 Voltage-current characteristic curves for initial stack temperatures of 28 and 44 °C

water-cooling system could be utilised. For example, an experimental fuel-cell-powered UAV developed by GTRI utilised water cooling [5]. Deionised water was pumped through the fuel cell and an air-cooled radiator. These alternative systems add mass to the aircraft; however, they are often unavoidable for higher-powered fuel cells.

This page is intentionally blank

6. Power Supply

Fuel cells require a number of powered devices for fuel and oxidant supply, thermal management and system control; and they generally utilise a portion of the power generated by the fuel-cell stack. In the experiments described in §3–5, the Hy-Expert system's BOP devices were powered by the mains-power grid. However, as described in this section, the Hy-Expert system was also tested in grid-independent mode. In this configuration, a battery is used for the initial start-up; and when the fuel-cell stack reaches a nominal operating condition, the system becomes self-sustaining. To provide the BOP devices with a fixed voltage, the Hy-Expert system utilises a voltage converter. Here, the effect of parasitic loads on the Hy-Expert system's power response and the power loss associated with voltage conversion are described.

6.1 Parasitic Load

The electrical circuit of the Hy-Expert system was modified from the arrangement of Figure 7 to that shown in Figure 17. In this configuration, the stack provided a variable voltage to the output load, as before; whilst the BOP devices were powered with a fixed voltage of 12 V through the use of a voltage converter.

Initially the total parasitic load, P_{BOP} , was measured with an output load of zero ($P_{out} = 0$). The results, given in Table 2, indicate that the fuel cell's BOP devices, including the airflow fans, LED displays, solenoid valve, control board, *etc.*, draw significant power. The stack output power, P_{stack} , was greater than the measured parasitic load. This is attributed to losses that occur in the circuit prior to the point at which the power for the parasitic load is

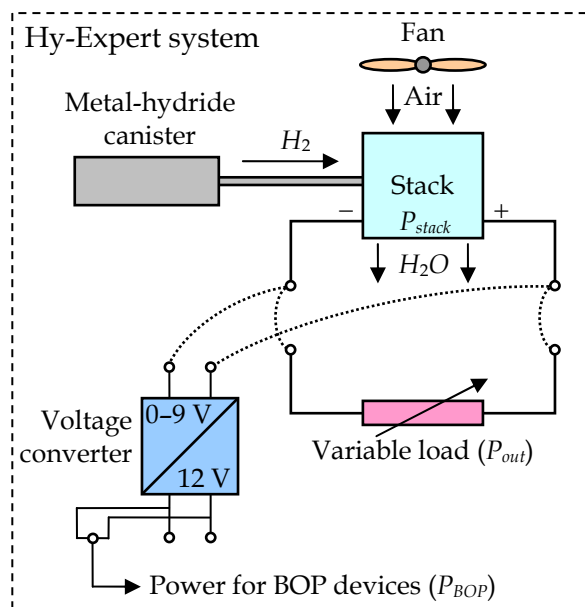


Figure 17 Layout of the Hy-Expert system in grid-independent mode, where the stack provides a variable voltage to the output load and a fixed voltage to the BOP devices

Table 2 Parasitic-load and stack power under no-load conditions, when the Hy-Expert system is operated in grid-independent mode

Parameter	Measured value
P_{out}	0 W
P_{BOP}	5.20 W
V_{stack}	7.59 V
I_{stack}	1.01 A
P_{stack}	7.67 W

measured, *e.g.*, in the voltage converter, in the sensor used to measure the stack current, and in the connecting cables.

The parasitic load was also measured as a function of stack current by varying the output load. The parasitic load increased gradually with the stack current (and power), as shown in Figure 18(a). The parasitic load can be divided into fixed and variable components. Peripherals such as the LED displays, solenoids and control board consume a fixed amount of power, regardless of the load. They draw ~ 5.2 W and are responsible for the non-zero parasitic load observed with a zero output load. In contrast, the power consumed by the cooling fans varies with stack current (and thus with the output load) and is responsible for the gradual increase in the parasitic load with increasing stack current.

A comparison of the power supplied by the stack in grid-independent mode and the power consumed by the output load is shown in Figure 18(b). As expected, the power to the load (P_{out}) is significantly less than that supplied by the stack (P_{stack}), because of the requirements of the BOP. The divergence of the curves with increasing power is due to the increase in internal requirements (*i.e.*, the demands of the cooling fans) with increasing stack current. The difference between the stack and output-load power levels does not correspond exactly to the measured parasitic load due to losses between the points where the stack current and voltage are monitored and where the parasitic load is measured.

It has been shown that a significant portion of the stack output power (even at 50 W) is consumed by BOP devices and by losses associated with supplying them (*e.g.*, the voltage converter). Given the typical desire to optimise energy usage on-board a fuel-cell-powered UAV, efforts are usually made to minimise the amount of power lost to parasitic loads. Several methods may be used, including: optimising the control system through more efficient software and hardware, minimising lead lengths in order to reduce line losses, and implementing a passive cooling system, rather than using fans. Consideration should also be given to the use of alternative energy sources altogether. For example, photovoltaic cells placed on the aircraft's external surfaces could be used to charge an on-board battery, which in turn could provide power for the BOP devices of the fuel-cell system.

6.2 Voltage-Conversion Losses

To quantify the losses associated with the voltage converter, the Hy-Expert system was placed in the configuration shown in Figure 19. As previously discussed, the voltage

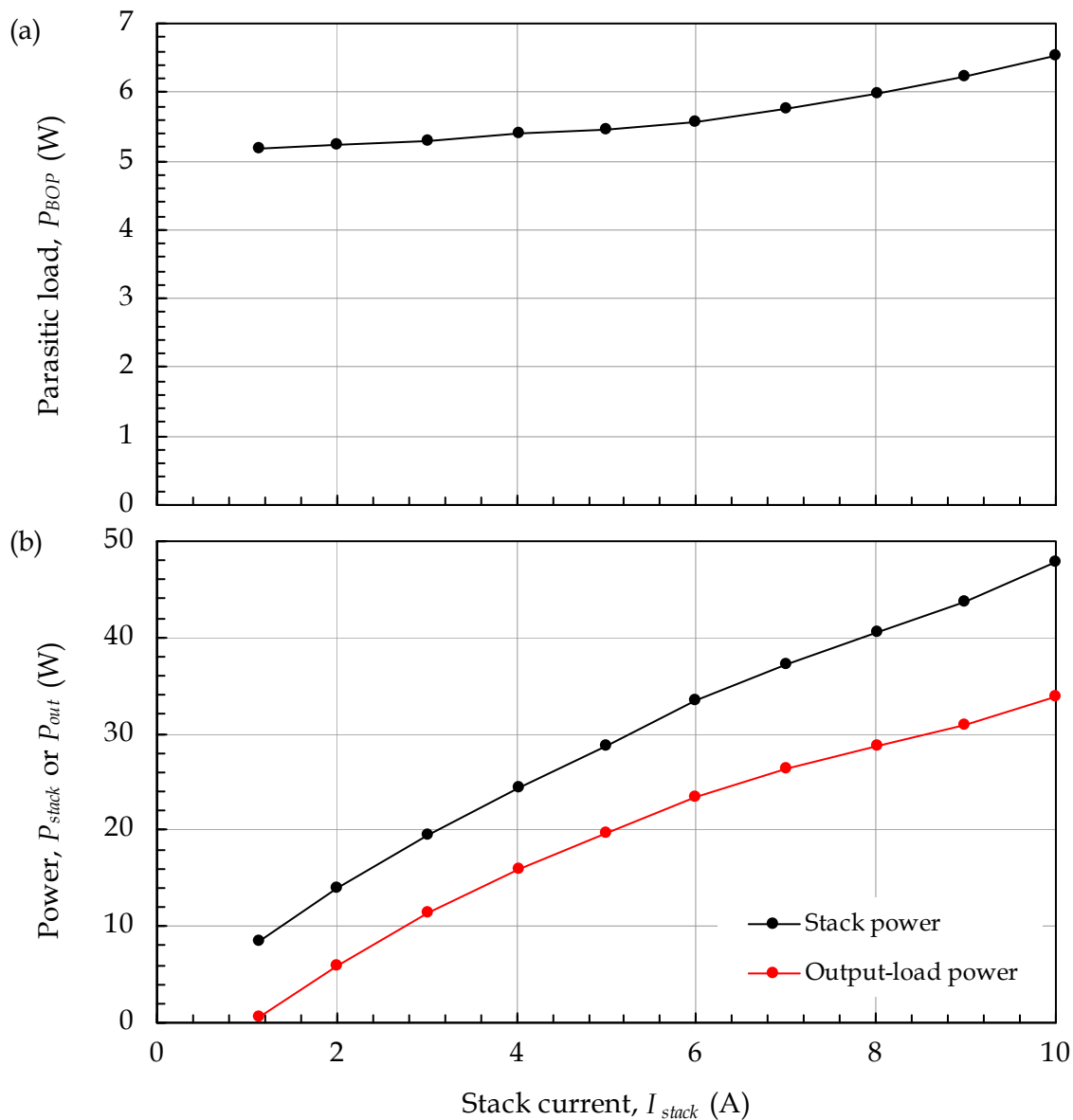


Figure 18 (a) Parasitic load and (b) output-load and stack power as functions of stack current when the Hy-Expert system is operated in grid-independent mode

converter was used to provide the necessary fixed voltage (12 V) to the BOP; and in this case it was used to supply both the BOP and the output load. The power response of the Hy-Expert system with the load driven via the voltage converter was compared with the results obtained with the output load powered directly by the fuel cell, at a variable voltage of 5–9 V (Figure 8(a)). The results are depicted in Figure 20. As expected, the power available at the output load was reduced when the voltage converter was used to supply a constant voltage not only to the BOP devices, but also to the output load. The loss at the rated output current of the fuel cell (8 A) was 3.6 W, a 13% reduction relative to the output-load power obtained with the stack supplying power directly to the output load (*i.e.*, without the converter supplying the load).

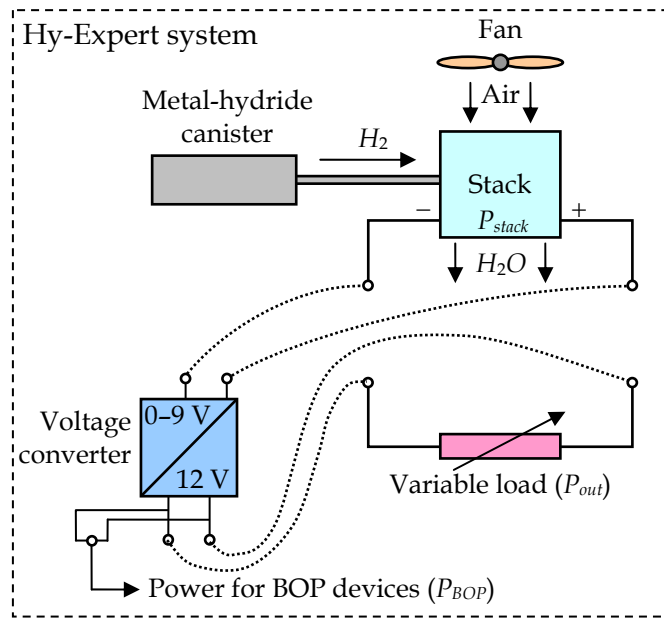


Figure 19 Layout of the Hy-Expert system in grid-independent mode, with the stack providing a fixed voltage to the output load and BOP devices

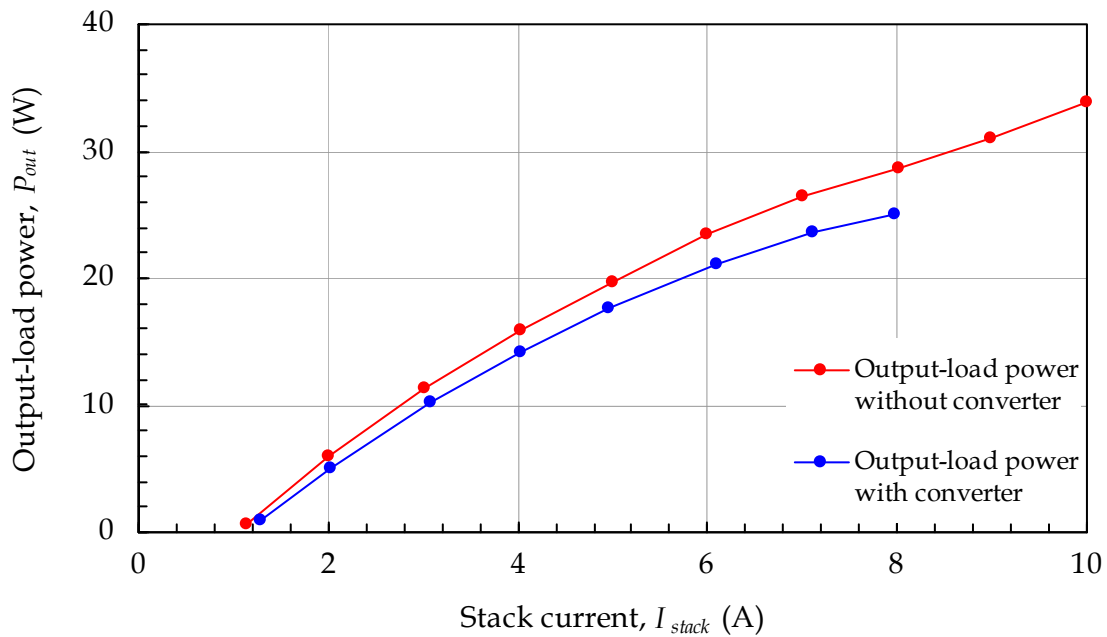


Figure 20 Output-load power as a function of current with and without voltage converter in the circuit

6.3 Power-Supply Efficiency

In §0, the stack efficiency was calculated for various output loads when the BOP devices of the system were powered by the mains-power grid. Here, the stack, system, and total effi-

ciencies of the system are described for the case when the fuel-cell system is self-sustaining (*i.e.*, the BOP devices are powered by the fuel cell via the voltage converter) and the output load is powered directly by the fuel cell, rather than via the voltage converter. The total efficiency of the Hy-Expert system was characterised to find its optimum operating point; and the stack and system efficiencies were determined.

6.3.1 Total Efficiency

The load current was varied between 0 and 10 A; and the stack voltage, hydrogen flow rate, and load power were measured at a number of points within this range. The total efficiency of the Hy-Expert system, η_{total} , can be calculated by use of an expression analogous to Equation (10) with P_{stack} replaced by P_{out} :

$$\eta_{total} = \frac{P_{out}}{LHV \cdot \dot{\mathcal{V}}_{H_2}} \quad (21)$$

The results, depicted in Figure 21, indicate a maximum total efficiency of ~31%, at an output load of 15–20 W. This value is significantly less than the maximum stack efficiency of the non-self-sustaining arrangement discussed in §4.1 ($\eta_{stack} = 55\%$). Furthermore, the optimum working range appears to be above 10 W, where the total efficiency is 27–31%.

6.3.2 Stack and System Efficiency

The total efficiency may be decomposed into the stack and system efficiencies (η_{stack} and η_{sys} , respectively), as follows:

$$\eta_{total} = \eta_{stack} \cdot \eta_{sys} \quad (22)$$

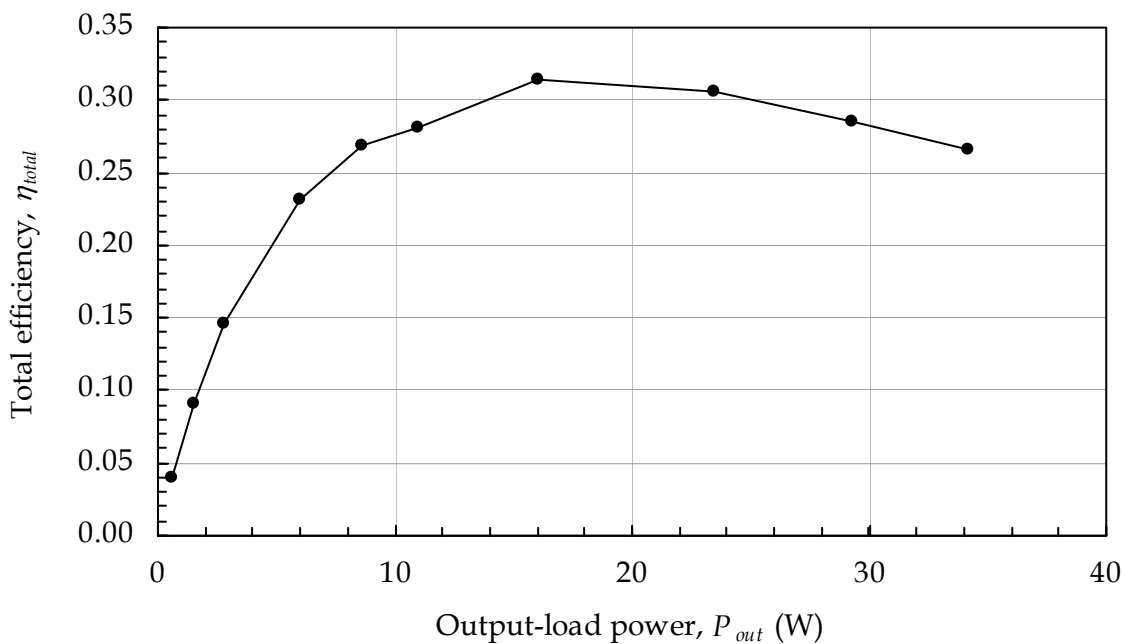


Figure 21 Total efficiency as a function of output-load power

The stack efficiency, as before, is the ratio of the stack power to the power input by the flow of reactants into the system, as shown by Equation (10); and the system efficiency is given by:

$$\eta_{sys} = \frac{P_{out}}{V_{stack} \cdot I_{stack}}. \quad (23)$$

Equations (10) and (23) were used to compute the stack and system efficiencies from the measured stack voltage and current, hydrogen flow rate, and output-load power; and the results are depicted in Figure 22.

The stack efficiency is the proportion of energy not lost to irreversibilities within the fuel-cell stack (including activation over-voltage, Ohmic losses, concentration losses, and losses associated with fuel crossover and internal currents) and, as shown in Figure 12, has a maximum at a stack power of zero. As described in §6.1, because the stack is supplying power to the BOP devices, its power is nonzero even when the main output load is disconnected and the power delivered to it is zero. Therefore, the stack efficiency curve is effectively shifted to lower output-load-power levels. Coincidentally, the magnitude of the shift means that the peak stack efficiency (~55%) corresponds approximately to an output-load power of zero (at which point all of the power from the stack is used by the BOP or lost within the system).

The system efficiency indicates the proportion of the stack power available to the output load (*i.e.*, the portion not lost to parasitic loads and irreversibilities external to the stack). As can be seen in Figure 22, the system efficiency increases with the magnitude of the output load, and the maximum efficiency (~70%) occurs at output loads of 24 W or more.

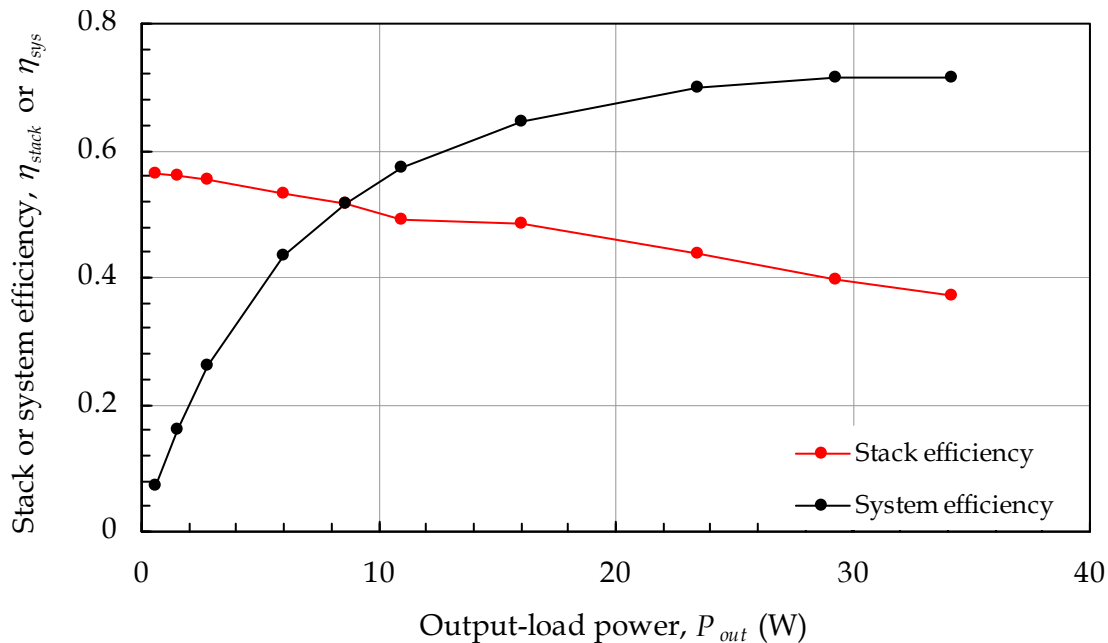


Figure 22 Stack and system efficiencies as functions of output-load power

7. Conceptual Fuel-Cell-System Design

To provide an example of basic fuel-cell design, a fuel cell suitable to power a small UAS was considered. The equations presented in §3 and §5 were used to determine the characteristics of the fuel-cell stack and the reactant requirements for a typical UAS mission.

7.1 Stack Size

The fuel cell was assumed to be rated to 500 W ($= P_{stack,max}$) and to have a working voltage of 24 V ($= V_{stack}$). Further, it was assumed that the values of cell voltage and current density calculated for the Hy-Expert stack, described in §3.2.1, were valid for this larger fuel cell (*i.e.*, $V_{cell} = 0.45$ V and $\rho_{cell} = 0.4$ A/cm², respectively).

The current, $I_{stack,max}$, at the rated stack power, $P_{stack,max}$, may be determined from the expression, $I_{stack,max} = P_{stack,max} / V_{stack}$, to be 20.8 A. The number of cells needed to produce the desired stack voltage was determined by solving Equation (2) for *no.cells* and inserting the appropriate values of stack and cell voltage (24 V and 0.45 V, respectively). The required number of cells was found to be 53. The active cell-surface area required to produce the desired stack (or cell) current was found to be 52 cm², by use of Equation (3) with the cell current density taken to be that of the Hy-Expert stack's cells.

The mass of the fuel-cell stack is also an important parameter for aircraft applications. It has not been estimated here because the specific power of a smaller fuel cell is not transferable to a larger fuel cell, which would be expected to have, *e.g.*, a smaller mass fraction for packaging and BOP devices. A simple method sufficed here to produce reasonable approximations of the required number of cells and active cell-surface area for given values of output stack power and voltage; however, a more thorough examination would be needed to provide a reasonable estimate of the fuel cell's mass.

7.2 Reactant Requirements

7.2.1 Hydrogen Flow Rate

For a given application, Faraday's laws may be used to estimate the required volume and flow rate of hydrogen gas to the fuel-cell stack considered here. One may insert *no.cells* = 53, $I_{th} = 21$ A, and $z_{H_2} = 2 e^- / \text{ion}$ into Equation (16) to determine the required hydrogen flow rate. This yields $\dot{V}_{H_2} = 7.8$ ℓ/min or 150 ml/min/cell, at standard conditions. Because the hydrogen flow rate increases proportionally with stack current near the fuel cell's optimal operating point, one may obtain the required volume of hydrogen gas at standard conditions by multiplying the flow rate by the operating time. For an 8-h mission, a volume of 3700 ℓ at standard conditions or 0.33 kg of hydrogen is obtained.

A computation of this sort may be used to select a hydrogen-gas cylinder or other storage device appropriate for a given mission. Furthermore, an on-board power-management system could utilise such data to determine whether to conserve or to use energy at

different stages in the mission. In the case where the consumption of hydrogen exceeds the average flow rate needed to reach the desired 8-h flight time, the power-management system may alter the mission plan of the UAS to bypass non-critical mission targets in order to conserve energy. On the other hand, if hydrogen usage has been significantly lower than that required to meet the 8-h flight time, for an extended period of time, the power-management system may permit the UAS to use more energy to meet additional mission targets or to fly at a higher airspeed.

7.2.2 Oxygen-Flow and Airflow Rates

As was done for hydrogen, the airflow rate required to meet the demands of the load was estimated. Values of $no.cells = 53$, $I_{th} = 21$ A, and $z_{O_2} = 4 e^- / ion$ were inserted into Equation (19); and the required oxygen flow rate, \dot{V}_{O_2} , was found to be 3.9 mL/min at standard conditions. This is half the required volumetric flow rate of hydrogen, because the product, water, contains two hydrogen atoms for each oxygen atom. Equation (20) then yielded a total airflow rate, \dot{V}_{air} , of 19.3 L/min for the 53-cell stack. This equates to a total volume of 9300 mL at standard conditions or 6.6 kg of air for an 8-h mission. This volume is only the amount of air needed for the reaction and does not include any excess air. If only the flow rate required for the reaction were supplied, concentration losses at the cathode would likely result in the reaction being restrained. Furthermore, the air volume computed here does not include air for cooling.

Similarly, the flow rate of water vapour formed during the reaction was determined by use of a relation analogous to Equations (16) and (19) for hydrogen and oxygen, respectively. The valency of water, z_{H_2O} , is $2 e^- / ion$; thus, the rate of formation of water at a load current of 21 A was found to be 7.8 L/min or 150 mL/min/cell.

8. Conclusion

This report documents the experimental characterisation of the Hy-Expert fuel-cell system. Although the Hy-Expert system exhibits similar characteristics to larger systems, it is not suitable for UAS applications. However, the experiments described here provide valuable insight into the fundamental mechanisms of PEM fuel-cell operation and the various issues that are relevant to UAS applications.

Various findings made throughout the report regarding the implementation of a fuel-cell system on-board a UAV are summarised below.

- The components needed to operate a fuel-cell stack and to supply it with reactants (the balance of plant making up the complete fuel-cell system) add mass and volume to the powerplant that typically make the specific power (power per unit mass) lower than that of traditionally fuelled powerplants (*e.g.*, internal-combustion engines) or battery-powered systems (*i.e.*, electric motors and batteries). However, the great advantage of fuel-cell-based powerplants is their specific energy (energy per unit mass), which can be superior to that of other powerplant types. It is this property of fuel-cell systems that makes them attractive candidates for powering UAVs, because of the increases in range and endurance that their higher specific energy can provide.
- Irreversibilities inherent to fuel-cell stacks create a dependence of output voltage on load current; and this poses a significant issue for implementing a fuel cell onto a UAV. A voltage converter or some external fixed-voltage source, such as a battery, is needed to power electrical loads requiring constant input voltages, such as payloads, avionics, and communications equipment. The devices required to control and provide reactants for the fuel-cell stack also require a fixed-voltage source. The presence of a voltage regulator or an additional power source, however, will incur additional electrical losses and add mass to the system.
- Several of the irreversibilities of fuel-cell stacks may be reduced by operating at higher temperatures than the usual 40 °C at which, *e.g.*, the Hy-Expert stack operates. Increasing the operating temperature would also increase the stack's fuel efficiency; however, this would increase the start-up time of the fuel cell, which may be undesirable for UAS applications. Furthermore, the commensurate increase in the thermal signature of the UAV could be detrimental to mission performance and survivability.
- The efficiency and specific power of a fuel-cell stack may be enhanced through improvements to the manufacturing process, though these are likely to increase the cost and potentially decrease the durability of the stack.

- A non-self-sustaining fuel-cell stack attains its optimum efficiency at relatively low loads (~1 A for the Hy-Expert system). For UAS applications, it may be practical to sacrifice fuel efficiency by operating near the fuel cell's maximum power. If stack efficiency were to be optimised, a fuel cell with a greater power rating (and therefore larger physical size and mass) would be required.
- Self-sustaining fuel-cell systems exhibit lower overall efficiency due to the additional power consumed by devices required to control the fuel cell and to provide reactants (balance-of-plant devices). In this case, however, the optimum efficiency occurs at relatively higher loads, providing an advantage for UAS applications. Alternatively, the additional devices can be powered by an external power source such as a battery, which has the additional advantage of supplying a fixed voltage.
- Faraday's laws can be used to predict the amounts of hydrogen and oxygen needed for a particular mission with a desired average load current and duration. The effect of lower atmospheric air density with increasing altitude may be important, depending on the mission profile.
- Temperature and water management are significant issues in high-powered PEM fuel cells (system producing > 100 W). Simple fan cooling of the stack, such as is employed by the Hy-Expert system, is likely to be insufficient for UAS applications requiring high power. Instead, the use of a more complex setup including an air moisturiser (to prevent drying of the PEM) or water cooling system is required. These additional devices are likely to add weight to the aircraft and to consume more space on-board.

Complementary work in the Strategic Research Initiative project on "Hybrid-Propulsion and Power-Management Technologies for Tactical Unmanned Aircraft Systems (UAS)" includes the development of a hardware-in-the-loop testing facility to characterise and compare the performance of various fuel-cell technologies available on the market. While only PEM fuel cells have been considered here, investigations into the peculiarities of other fuel-cell types (*e.g.*, alkaline-electrolyte, direct-methanol, and sulphur-oxide fuel cells) are also required so that a broad assessment of fuel-cell types and their likely performance on UAS can be derived.

References

1. Bradley, T.H., and D.E. Parek, Comparison of design methods for fuel-cell-powered unmanned aerial vehicles. *Journal of Aircraft*, November–December 2009, **46**(6): pp. 1945–1956.
2. Larminie, J., and A. Dicks, *Fuel cell systems explained*. 2nd ed. 2003, John Wiley and Sons Ltd.: Chichester, West Sussex, England. p. 418. Available from: www.iitk.ac.in/erl/Index_files/home_files/Refrence%20Book.pdf [cited 23 August 2013].
3. Cook, B., *An introduction to fuel cells and hydrogen technology*. December 2001, Heliocentris Fuel Cells AG and Heliocentris Energiesysteme GmbH: Vancouver, BC, Canada. p. 28. Available from: <http://www.fuelcellstore.com/products/heliocentris/INTRO.pdf> [cited 23 August 2013].
4. Boscaino, V., G. Capponi, P. Livreri, and F. Marino, Fuel cell modelling for power supply systems design in *11th IEEE Workshop on Control and Modeling for Power Electronics*, 17–20 August 2008, Zurich, Switzerland. IEEE: Piscataway, NJ, USA. Available from: http://www.st.com/st-web-ui/static/active/jp/resource/technical/document/conference_paper/04634671.pdf [cited 23 August 2013].
5. Bradley, T.H., B.A. Moffitt, D.N. Mavris, and D.E. Parekh, Development and experimental characterization of a fuel cell powered aircraft. *Journal of Power Sources*, 27 September 2007, **171**(2): pp. 793–801. Available from: http://www.engr.colostate.edu/~thb/Publications/JPS_FCUAV.pdf [cited 23 August 2013].
6. LaBreche, T., and N. Ernst, Advanced hybrid fuel cell power systems for UAVs. Paper 1890 in *Proceedings of the AUVSI Unmanned Systems North America Conference*, Vol. 2, 11–13 August 2009, Washington, DC, USA. Association for Unmanned Vehicle Systems International, pp. 638–641.
7. Cai, Q., D.J.L. Brett, D. Browning, and N.P. Brandon, A sizing-design methodology for hybrid fuel cell power systems and its application to an unmanned underwater vehicle. *Journal of Power Sources*, 1 October 2010, **195** (19): pp. 6559–6569. Available from: <http://www.sciencedirect.com/science/article/B6TH1-4YYXJNY-4/2/f8bb75a8e39888a5961e3f988c180fb3> [cited 23 August 2013].
8. Jeong, K.S., and B.S. Oh, Fuel economy and life-cycle cost analysis of a fuel cell hybrid vehicle. *Journal of Power Sources*, 5 March 2002, **105** (1): pp. 58–65. Available from: <http://www.sciencedirect.com/science/article/B6TH1-44J6K98-2/2/09228b3a1128fcd200acc8a9c03f8e21> [cited 23 August 2013].

9. Lapeña-Rey, N., J. Mosquera, E. Bataller, F. Ortí, C. Dudfield, and A. Orsillo, Environmentally friendly power sources for aerospace applications. *Journal of Power Sources*, 1 July 2008, **181**(2): pp. 353–362.
10. Bernay, C., M. Marchand, and M. Cassir, Prospects of different fuel cell technologies for vehicle applications. *Journal of Power Sources*, 1 June 2002, **108**(1–2): pp. 139–152. Available from: http://www.researchgate.net/publication/223311655_Prospects_of_different_fuel_cell_technologies_for_vehicle_applications/file/60b7d51b0b0c0bc7a6.pdf [cited 23 August 2013].
11. Granovskii, M., I. Dincer, and M.A. Rosen, Economic and environmental comparison of conventional, hybrid, electric and hydrogen fuel cell vehicles. *Journal of Power Sources*, 22 September 2006, **159** (2): pp. 1186–1193. Available from: <http://www.sciencedirect.com/science/article/B6TH1-4J2M1S8-2/2/ecd82072151b9c00f4017436e05b6276> [cited 23 August 2013].
12. Flightglobal, Reed Business Information, *Down sizing*, 25 October 2005. Available from: <http://www.flightglobal.com/articles/2005/10/25/202326/down-sizing.html> [cited 18 August 2011].
13. Palmer, J.L., Assembly and initial analysis of a database of the characteristics and performance of unmanned aerial systems, April 2014, Report DSTO-TR-2952, Aerospace Division, Defence Science and Technology Organisation, Fishermans Bend, VIC, Australia.
14. Horizon Energy Systems, Pte. Ltd., *Horizon's fuel cell triples flight duration capability of South Korean close-range UAV*, 9 November 2010. Available from: <http://www.hes.sg/files/AEROPAKkari.doc> [cited 18 August 2011].
15. *Jane's Unmanned Aerial Vehicles and Targets*, 2013. Available from: http://catalog.janes.com/catalog/public/index.cfm?fuseaction=home.ProductInfoBrief&product_id=98136 [cited 23 August 2013].
16. Uconsystem Corp., *Unmanned aerial vehicle (RemoEye-006)*, 2013. Available from: http://uconco.en.ec21.com/Unmanned_Aerial_Vehicle_RemoEye_006--865587_866976.html [cited 23 August 2013].
17. Sadden, E., *The exciting potential of fuel cell-powered UAVs*, FuelCellWorks, 17 January 2011. Available from: <http://fuelcellsworks.com/news/2011/01/17/the-exciting-potential-of-fuel-cell-powered-uavs/> [cited 23 August 2013].
18. World's first commercial fuel cell unmanned aerial system. *GizMag*, 6 August 2009. Available from: <http://www.gizmag.com/worlds-first-commercial-fuel-cell-unmanned-aerial-system/12453/> [cited 23 August 2013].

19. *Boomerang: Long endurance, fuel-cell powered mini UAV*, 2009. Available from: http://www.bluebird-uav.com/Products_Boomerang.html [cited 18 August 2011].
20. Mortimer, G., AeroVironment Puma small UAS achieves record flight of over nine hours using fuel cell battery hybrid system. *sUAS News*, 6 March 2008. Available from: <http://www.suasnews.com/2008/03/3301/aerovironment-puma-small-uas-achieves-record-flight-of-over-nine-hours-using-fuel-cell-battery-hybrid-system/> [cited 23 August 2013].
21. Aerovironment, Inc., *Puma AE overview*, 2010. Available from: http://www.avinc.com/downloads/PumaAE_0910.pdf [cited 23 August 2013].
22. Hewish, M., A bird in the hand. *Jane's International Defence Review*, 1 November 1999, **32**(11). Available from: <https://janes.ihs.com/CustomPages/Janes/DisplayPage.aspx?DocType=News&ItemId=+++1099348&Pubabbrev=IDR> [cited 23 August 2013].
23. Kellogg, J.C., C. Bovais, R.J. Foch, H. McFarlane, C. Sullivan, J. Dahlburg, J. Gardiner, R. Ramamurti, D. Gordon-Spears, R. Hartley, B. Kamgar-Parsi, F. Pipitone, W. Spears, A. Sciambi, and D. Srull, The NRL Micro Tactical Expendable (MITE) air vehicle. *Aeronautical Journal*, August 2002, **106**(1062): pp. 431-441.
24. Kellogg, J.C., L. Monforton, D. White, M. Vick, K. Swider-Lyons, and P. Bouwman, Fuel cells for micro air vehicles. Presented at *Joint Service Power Expo*, 2-5 May 2005, Tampa, FL, USA: National Defense Industrial Association: Arlington, VA, USA. Available from: http://proceedings.ndia.org/5670/Fuel_Cells-Kellogg.ppt#286 [cited 19 February 2013].
25. Micro air vehicle flies under fuel cell power. *Jane's International Defence Review*, 13 June 2003. Available from: <https://janes.ihs.com/CustomPages/Janes/DisplayPage.aspx?DocType=News&ItemId=+++1102117&Pubabbrev=IDR> [cited 23 August 2013].
26. Unmanned aerial vehicles and drones. *Aviation Week & Space Technology*, 28 January 2008, **168**(1): pp. 114-122.
27. LaBreche, T., Solid oxide fuel cell power systems for small UAVs in *Joint Service Power Expo*, 24-26 April 2007, San Diego, CA, USA. Defense Technical Information Center.
28. Barnard Microsystems, Limited, *Korean scientists build fuel cell-powered unmanned aircraft*, 2007. Available from: http://www.barnardmicrosystems.com/L4E_fuel_cell_flight.htm [cited 18 August 2011].
29. Patel, N., Korean researchers build a fuel cell UAV that runs for 10 hours. *engadget*, 17 October 2007. Available from: <http://www.engadget.com/2007/10/17/korean-researchers-build-a-fuel-cell-uav-that-runs-for-10-hours/> [cited 18 August 2011].

30. Hannover Fair, *Fochhochschule Weisbaden, University of Applied Sciences*, 2005. Available from: <http://www.hydrogenambassadors.com/hm05/exhibitors/fh-wiesbaden.php> [cited 23 August 2013].
31. Hannover Fair, *Hy-Fly der Wasserstoffflieger*, 2005. Available from: <http://www.hydrogenambassadors.com/hm05/forum/fh-wiesbaden.php> [cited 23 August 2013].
32. Moffitt, B.A., Design and hardware validation of a 24 hour endurance fuel cell UAV. Presented at *16th Annual External Advisory Board Review*, 30 April - 1 May 2008, Atlanta, GA, USA: Georgia Institute of Technology. Available from: http://www.phoenix-int.com/GTsymposium/April30/8_Moffitt.pdf [cited 19 February 2013].
33. Kellogg, J.C., *Fuel cell propulsion for small UAVs*, November 2005. Available from: <http://www.nrl.navy.mil/techtransfer/exhibits/uavinfosht.html> [cited 22 August 2008].
34. Atkins, D., and B.A. Moffitt, PEM fuel cell powered demonstrator UAV in 2006 *NASA/DoD URETI on Aeropropulsion and Power Technology (UAPT) Program Review*, 10-12 October 2005, Tallahassee, FL, USA. Georgia Institute of Technology. Available from: http://www.asdl.gatech.edu/teams/ureti/AnnualReview2006/pdf/2.6_Education_PEM_FC_UAV.pdf [cited 19 May 2008].
35. Boland, R., Experimental power system expands flight capabilities. *SIGNAL Magazine*, March 2006. Available from: <http://www.afcea.org/signal/> [cited 14 April 2008].
36. University of Michigan students set new UAV record. *Fuel Cell Today*, 12 November 2008. Available from: <http://www.fuelcelltoday.com/news-events/news-archive/2008/november/university-of-michigan-students-set-new-uav-record> [cited 18 August 2013].
37. Kaz, T., *Successful first flight of the "HyFish" - a fuel cell model aircraft is in the air*, 3 April 2007. Available from: http://translate.google.com/translate?hl=en&sl=de&u=http://www.dlr.de/desktopdefault.aspx/tabid-4550/127_read-8329/&sa=X&oi=translate&resnum=2&ct=result&prev=/search%3Fq%3DErfolgreicher%2BERstflug%2Bdes%2Bhyfish%26hl%3Den [cited 23 August 2013].
38. Horizon Energy Systems, Pte. Ltd., *World's first zero emission, hydrogen fuel cell jet*, 6 April 2007. Available from: <http://www.horizonfuelcell.com/hyfish.htm> [cited 23 August 2013].
39. Mortimer, G., *Fuel cell long endurance platform for EnergyOR unveiled by Robota*, sUAS News, 12 August 2011. Available from: <http://www.suasnews.com/2011/08/6565/fuel-cell-long-range-platform-for-energyor-unveiled-by-robota/> [cited 18 August 2011].

40. EnergyOR fuel cell UAV achieves 10 hour flight endurance. *Fuel Cell Today*, 16 August 2011. Available from: <http://www.fuelcelltoday.com/news-events/news-archive/2011/august/energyor-fuel-cell-uav-achieves-10-hour-flight-endurance> [cited 18 August 2013].
41. Herwerth, C., U.C. Ofoma, C.C. Wu, S. Matsuyama, and S. Clark, Development of a fuel cell powered UAV for environmental research. Paper AIAA-2006-237 in *Technical Papers – 44th AIAA Aerospace Sciences Meeting*, Vol. 5, 9–12 January 2006, Reno, NV, USA. American Institute of Aeronautics and Astronautics, Inc.: New York, NY, USA, pp. 2851–2864.
42. Johnsen, F.A., California students join small circle of revolutionary fuel-cell fliers. *NASA Dryden Flight Research Center news*, 5 October 2006. Available from: http://www.nasa.gov/vision/earth/improvingflight/fuel_cells.html [cited 22 August 2008].
43. Warwick, G., *Fuel-cell mini UAV sets world distance record*, Flightglobal, 1 November 2007. Available from: <http://www.flightglobal.com/articles/2007/11/01/219093/fuel-cell-mini-uav-sets-world-distance-record.html> [cited 18 August 2011].
44. Georgia Tech Research Institute, *Flying on hydrogen: Georgia Tech researchers use fuel cells to power unmanned aerial vehicle*, 2006. Available from: <http://www.gtri.gatech.edu/casestudy/flying-hydrogen> [cited 18 August 2011].
45. Bradley, T.H., B.A. Moffitt, D.N. Mavris, and D.E. Parekh, Validated modeling and synthesis of medium-scale polymer electrolyte membrane fuel cell aircraft. Paper 2006-97233 in *Proceedings of FUELCELL2006, 4th International ASME Conference on Fuel Cell Science, Engineering and Technology*, 19–21 June 2006, Irvine, CA, USA. American Society of Mechanical Engineers: New York, NY, USA, pp. 381–390. Available from: http://www.engr.colostate.edu/~thb/Publications/FUELCELL2006_97233.pdf [cited 23 August 2013].
46. Moffitt, B.A., T.H. Bradley, D.E. Parekh, and D.N. Mavris, Design and performance validation of a fuel cell unmanned aerial vehicle. Paper AIAA-2006-823 in *Technical Papers – 44th AIAA Aerospace Sciences Meeting*, Vol. 13, 9–12 January 2006, Reno, NV, USA. American Institute of Aeronautics and Astronautics, Inc.: New York, NY, USA, pp. 9877–9896. Available from: www.engr.colostate.edu/~thb/Publications/AIAA-2006-0823.PDF [cited 23 August 2013].
47. Moffitt, B.A., T.H. Bradley, D.N. Mavris, and D.E. Parekh, Design space exploration of small-scale PEM fuel cell long endurance aircraft. Paper AIAA-2006-7701 in *Technical Papers – 6th AIAA Aviation Technology, Integration, and Operations Conference*, Vol. 1, 25–27 September 2006, Wichita, KS, USA. American Institute of Aeronautics and Astronautics, Inc.: New York, NY, USA, pp. 14–29. Available from: <http://www.engr.colostate.edu/~thb/Publications/ATIO%20Final%20as%20submitted.pdf> [cited 23 August 2013].

48. Bradley, T.H., B.A. Moffitt, D.E. Parekh, and D.N. Mavris, Flight test results for a fuel cell unmanned aerial vehicle. Paper AIAA-2007-32 in *Technical Papers – 45th AIAA Aerospace Sciences Meeting and Exhibit*, Vol. 1, 8–11 January 2007, Reno, NV, USA. American Institute of Aeronautics and Astronautics, Inc.: New York, NY, USA, pp. 254–261. Available from: www.engr.colostate.edu/~thb/Publications/AIAA_Testing_paper_v10.pdf [cited 23 August 2013].
49. Aerovironment Global Observer: The first hydrogen-powered unmanned flight. *Popular Science* 2005. Available from: <http://www.popsci.com/military-aviation-space/article/2005-11/aerovironment-global-observer> [cited 18 August 2011].
50. Flightglobal, Reed Business Information, *Aerovironment details new Global Observer variants*, 14 February 2006. Available from: <http://www.flightglobal.com/articles/2006/02/14/204655/aerovironment-details-new-global-observer-variants.html> [cited 18 August 2011].
51. Sweetman, B., Boeing working on new large UAV. *Jane's Defence Weekly*, 5 July 2006, 43(27): pp. 735–736.
52. Flightglobal, Reed Business Information, *UAV Directory – Aircraft specification: AeroVironment – Global Observer GO-1*, 5 July 2007. Available from: <http://www.flightglobal.com/directory/detail.aspx?aircraftCategory=UAV&manufacturerType=UAV&navigationItemId=374&aircraftId=7481&manufacturer=21926&keyword=&searchMode=Keyword&units=Imperial> [cited 18 August 2011].
53. Executive Overview: Unmanned aerial vehicles. *Jane's Unmanned Aerial Vehicles and Targets* 2011. Available from: http://catalog.janes.com/catalog/public/index.cfm?fuseaction=home.ProductInfoBrief&product_id=98136 [cited 18 August 2011].
54. Niles, R., *Boeing flies fuel cell aircraft*, 4 April 2008. Available from: http://www.avweb.com/avwebflash/news/BoeingFliesFuelCellAircraft_197531-1.html [cited 18 August 2011].
55. “Meister” wins 2010 Japan International Birdman Rally, 4 October 2010. Available from: http://www.titech.ac.jp/english/news-topics/detail_1402.html?id=news-topics [cited 18 August 2011].
56. *World's first battery-powered manned plane soars into the sky*, 2008. Available from: http://www.titech.ac.jp/english/about/introduction/outline2008-2009/pdf/0809outline_07.pdf [cited 18 August 2011].
57. *Antares 20E*, 2008. Available from: http://www.lange-flugzeugbau.com/htm/english/products/antares_20e/antares_20E.html [cited 26 August 2008].

58. Dunn, J.P., Electric Powered Aircraft – Part 1: Air fuel cells, the wave of the future for general aviation? *Kitplanes Magazine*, April 2002. Available from: <http://www.kitplanes.com/magazine/engines/178-1.phtml> [cited 3 September 2008].
59. Dunn, J.P., Electric Powered Aircraft – Part 3: Motor and propeller selection are the topics this time. *Kitplanes Magazine*, April 2003. Available from: <http://www.kitplanes.com/magazine/engines/176-1.phtml> [cited 3 September 2008].
60. Launie, P.T., and J.P. Dunn, Electric Powered Aircraft – Part 2: Selecting the right aircraft to electrify. *Kitplanes Magazine*, September 2002. Available from: <http://www.kitplanes.com/magazine/engines/177-1.phtml> [cited 3 September 2008].
61. Vorkoetter, S., *Demystifying full-scale electric powered airplanes*, April 2010. Available from: <http://www.stefanv.com/rcstuff/qf200404.html> [cited 18 August 2011].
62. *Reasons to choose a Silent 2 Targa*. Available from: http://www.alisport.com/eu/eng/silent2targa_scelta.htm [cited 18 August 2011].
63. *ElectraFlyer Trike*, 2009. Available from: <http://www.electraflyer.com/trike.php> [cited 18 August 2011].
64. Plug and fly: The battery-powered plane makes its debut. *Wired* 2008. Available from: <http://blog.wired.com/cars/2008/08/the-company-cla.html> [cited 18 August 2011].
65. *All-electric ElectraFlyer C takes flight at the Oshkosh Air Show*, 2008. Available from: <http://www.nextenergynews.com/news08/next-energy-news8.4.08b.html> [cited 18 August 2011].
66. Pew, G., *APAME announces electric flight*, 29 December 2007. Available from: http://www.avweb.com/avwebflash/news/APAMEAnnouncesElectricFlight_196847-1.html?type=pf [cited 26 August 2008].
67. *First flights of electrical motor glider "Alatus"*, 2009. Available from: <http://www.apame.eu/AA%20Projects.html> [cited 18 August 2011].
68. *"Swift-Eye"*. Available from: <http://www.cyberflight.flyer.co.uk/swift.htm> [cited 18 August 2011].
69. *Taurus Electro*, 2010. Available from: <http://www.pipistrel.si/plane/taurus-electro/overview> [cited 18 August 2011].
70. *Taurus Electro technical data*, 2010. Available from: <http://www.pipistrel.si/plane/taurus-electro/technical-data> [cited 18 August 2011].
71. Moore, M.D., Electric propulsion enabled advanced air vehicles. Presented at *Electric Aircraft Symposium*, 26 April 2008 2008, San Francisco, CA, USA: CAFE Foundation,

- Santa Rosa, CA, USA. Available from: http://cafefoundation.org/v2/pdf_pav_electricaircraft/2008/mark.moore.eas2008.pdf.
72. *Taurus ELECTRO is flying!*, 21 December 2007. Available from: <http://www.pipistrel.si/news/739> [cited 22 August 2008].
73. *ElectraFlyer brochure*, 2009. Available from: http://www.electraflyer.com/forms/electraflyer_brochure.pdf [cited 18 August 2011].
74. Coppinger, R., *Prototype flight success could see French all-electric GA product*, 11 January 2008. Available from: <http://www.flightglobal.com/articles/2008/01/11/220729/prototype-flight-success-could-see-french-all-electric-ga.html> [cited 18 August 2011].
75. *ElectraFlyer C-Prototype*, 2009. Available from: <http://www.electraflyer.com/trike.php> [cited 18 August 2011].
76. *Electric-glider (Motoplaneur électrique) Alatus ME*, 10 January 2009. Available from: <http://www.electravia.fr/alatus.php> [cited 18 August 2011].
77. *E-Flight electric Waix achieves first flight*, 2010. Available from: http://www.sonexaircraft.com/press/releases/pr_120310.html [cited 18 August 2011].
78. *e-Flight Initiative*, 2011. Available from: <http://www.sonexaircraft.com/research/e-flight/> [cited 18 August 2011].
79. Lapeña-Rey, N., J. Mosquera, E. Bataller, and F. Ortí, Rey The Boeing fuel cell demonstrator airplane. Paper 2007-01-3906 in *Proceedings of the SAE 2007 Aerotech Congress & Exhibition*, 17–20 September 2007, Los Angeles, CA, USA. SAE International. Available from: <http://papers.sae.org/2007-01-3906/> [cited 23 August 2013].
80. *Battery-powered plane: World's first manned flight on dry cell batteries*, 29 September 2006. Available from: <http://web-japan.org/trends/science/sci060929.html> [cited 22 August 2008].
81. *Rapid 200*. Available from: <http://www.pilotmix.com/index.php?pgid=11&lang=en&maxInfo=811> [cited 18 August 2011].
82. Romeo, G., I. Moraglio, and C. Novarese, ENFICA-FC: Preliminary survey & design of 2-seat aircraft powered by fuel cells electric propulsion. Paper AIAA-2007-7754 in *Technical Papers — 7th AIAA Aviation Technology, Integration, and Operations Conference*, Vol. 1, 18–20 September 2007, Belfast, Northern Ireland. American Institute of Aeronautics and Astronautics, Inc.: New York, NY, USA, pp. 602–616.
83. *Jihlavan Airplanes: Touch the sky...Make your dreams come true*, 2008. Available from: <http://www.ultralight.cz/index.html> [cited 22 August 2008].

84. EG&G Technical Services, Inc., *Fuel cell handbook (7th edition)*. November 2004, U.S. Department of Energy, National Energy Technology Laboratory: Morgantown, WV, USA. Available from: <http://www.netl.doe.gov/technologies/coalpower/fuelcells/seca/pubs/FCHandbook7.pdf> [cited 23 August 2013].
85. *Heliocentris*, 2008. Available from: http://www.heliocentris.com/en/no_cache/homepage.html [cited 22 July 2008].
86. Heliocentris Energiesysteme GmbH, *Experiments guide and componenets description for the Hy-Expert Instructor Fuel Cell System*. 2005: Berlin, Germany. Available from: http://www.heliocentris.com/fileadmin/user_upload/02_Technical_Education/Instructor_Training_System/Experimente/Fuel-Cell-Trainer-Experiment-Guide.pdf [cited 23 August 2013].
87. Ramani, V., Fuel cells. *The Electrochemical Society Interface*, 2006, **15**(1): pp. 41-44. Available from: http://www.electrochem.org/dl/interface/spr/spr06/if_spr06.htm [cited 23 August 2013].
88. U.S. Department of Energy, Energy Efficiency and Renewable Energy, *Fuel cells*, 3 August 2011. Available from: http://www1.eere.energy.gov/hydrogenandfuelcells/fuelcells/fc_types.html [cited 23 August 2013].
89. Spiegel, C., *PEM fuel cell modeling and simulation using MATLAB™*. June 2008, Academic Press: Waltham, MA, USA. p. 456. Available from: <http://www.sciencedirect.com/science/book/9780123742599> [cited 23 August 2013].
90. Asselin, M., *An introduction to aircraft performance*. Education Series, Przemieniecki, J.S. Editor. 1997, American Institute of Aeronautics and Astronautics, Inc.: Reston, VA, USA.
91. Aerovironment flies world's first liquid hydrogen-powered UAV. *Space War: Your World at War*, June 2005. Available from: http://www.spacewar.com/reports/AeroVironment_Flies_Worlds_First_Liquid_Hydrogen_Powered_UAV.html [cited 23 August 2013].
92. ESDU International, *ESDU 77022, Equations for calculation of International Standard Atmosphere and associated off-standard atmospheres*, 1986. Available from: http://www.esdu.com/cgi-bin/ps.pl?sess=unlicensed_1130814010556bzh&t=doc&p=di_77022c [cited 23 August 2013].

Acknowledgements

The authors wish to thank Mr. Stuart Riddell, who was a member of DSTO's Maritime Platforms Division, for his assistance in designing the procedures for handling hydrogen gas and in creating the Work Health and Safety Documentation for this project. We also wish to acknowledge the contributions of Mr. Geoff Brian, the science-team leader of the project on "Hybrid-Propulsion and Power-Management Technologies for Tactical Unmanned Aircraft Systems (UAS)" under DSTO's Strategic Research Initiative on Signatures, Materials, and Energy, as well as Mr. Jan Drobik and Mr. Kevin Gaylor, who oversee projects in the Initiative's Energy stream.

Appendix A: Work Health and Safety Documents

DSTO Occupational Health and Safety Safe Operating Procedure: Use of Hy-Expert Instructor Fuel Cell System

Name of Equipment/Product: Hy-Expert Instructor Fuel Cell System

Division/Units: Maritime Platforms Division and Air Vehicles Division

Prepared By: James Harvey

Date: 22 February 2010

Approved By: Stuart Riddell

Date: 23 February 2010

The following OHS Safe Operating Procedure has been prepared for instruction to employees using the Hy-Expert Instructor Fuel Cell System.

1. Background/Equipment

This Safe Operating Procedure refers to the use of the Hy-Expert Instructor Fuel Cell System in Laboratory M2.76 of Building 94. The equipment in use includes the Fuel Cell Module FC50 (including power supply, control software, documentation), the Electronic Load Module EL200, the Voltage Converter Module VC100 and Ovonic's 2.2 kg Metal Hydride storage canister with refilling kit.

1.1 Personnel

One person with appropriate training and background is to be present at all times during the operation of the Hy-Expert Instructor Fuel Cell System.

1.2 Miscellaneous equipment

- Hy-Expert Instructor Fuel Cell System Operation Guide
- Fire extinguisher: Class D and CO₂
- Dry Sand
- Leak Detector Solution

2. Handling

- Eye protection to be worn at all times
- Ignition sources to be kept at safe stand-off distance

- Ensure correct polarity when making electrical connections
- Keep fingers away from fan housing
- At least one person is to be present during the fuel cell's operation

2.1 Personal Protection Equipment

- Safety glasses, goggles or face shield for eye protection
- Appropriate personal attire

3. Competency Assessment

Only personnel listed in the following table are authorised to operate the Hy-Expert Instructor Fuel Cell System.

Personnel	Assessment Date
Stuart Riddell	
James Harvey	18/02/2010

4. Document Review

This document is to be reviewed and re-approved every 12 months.

Review Date: 22 February 2011

5. Emergency Procedures

Only fight fire with hand held appliances if safe to do so.

6. Emergency Contact Details

- The emergency telephone number: 68888
- Local First Aiders: Harry Clark, Andrew McClean
- The location of the nearest First Aid Kit: Opposite Room M2.74

7. Occupational Health and Safety – Resources and Assistance

- DSTO OHS homepage
http://web-sa/workareas/OHS/new_home/home_page.shtml
- DSTO OH&S Site – Safe Work – Workshop
<http://web-vic.dsto.defence.gov.au/workareas/OHS/safe-work/workshop.shtml>
- Occupational Health, Safety & Compensation Branch (OSHC)
<http://ohsc.defence.gov.au/>

8. References

[1] Operating Guide – Hy-Expert Instructor Fuel Cell System 5th Edition 2005 Heliocentris Energiesystems GmbH

Installation

1. Check that the ventilation equipment in the laboratory is operating correctly. This can either be the fume hood or the air extraction trunk located above the “corridor” work bench.
2. Check that the ambient temperature is between +5°C and +35°C.
3. Ensure the fire extinguishers (Class D and CO₂) and the bucket of dry sand are positioned conveniently.
4. Ensure the test frame is installed on a stable, horizontal and solid base and that it stands firm.
5. Place the FC50 panel into the upper right area of the support frame and the EL200 panel into the lower right area of the test frame. Ensure they are held firmly within the frame.
6. Plug the connection cable of the 12V DC regulated power supply into the “12V=” jack of the FC50 and plug the power supply into an AC power outlet.
7. Connect the EL200 to the AC power outlet and turn on the power switch located behind the front plate on the right side. At this stage make sure the front panel switch is off.
8. Using the supplied test leads, connect the EL200 electronic load to the stack power output. **Note: Observe correct polarity.**
9. At this stage ensure the potentiometer is set to zero.
10. Attach the hydrogen supply with the quick coupler to the hydrogen input of the FC50. Ensure the coupler clicks cleanly into place and that the canister is held firmly to the support frame using the supplied clamping mechanisms.
11. Connect the control cable of the solenoid valve to the FC50.

Use of VC100 Voltage Converter Module VC100

The VC100 can be used such that the fuel cell system is grid independent. In this case:

- Fix the VC100 in the bottom left area of the frame.
- Connect the “12V=” jack of the FC50 to the 12V parasitic load output via the connection cable. (This is done in place of step 6.) **Note: Observe correct polarity.**
- Either the output of the FC50 can be connected to the EL200 input or the output of the VC100 can be connected to the EL200 input. **Note: Observe correct polarity.**

Start-up

12. Turn the hydrogen tap on (approximately 1.5 turns in an anti-clockwise direction) Ensure the canister pressure is greater than 1 bar. If not it must be refilled.
13. If necessary, squirt a leak detecting solution over the hydrogen pipe connections to check for leaks.
14. Turn the toggle switch on the front panel of the EL200 on.
15. Ensure the fan knob is set to "AUTO" for start-up.
16. Turn the FC50 main switch on.
17. Press the green start button.
18. Check the "Hydrogen flow" display for any error messages and refer to the Hy-Expert Instructor Fuel Cell System Operation Guide^[1] for error definitions.
19. Ensure the fuel cell system is operating between 0.6 ± 0.1 bar gauge.

Shut-down

20. Turn the potentiometer of the EL200 to zero and set the toggle and main switches off.
21. Turn the fan power knob to "AUTO" and turn the FC50 main switch off.
22. Turn the hydrogen tap off in a clockwise direction. To prevent damaging the tap thread, do not turn off too tightly.
23. Disconnect the hydrogen canister via the quick coupler.

Safety precautions in an emergency

Significant hydrogen escape

- Do not operate electrical devices, light switches, etc. as an explosive gas mixture could be present in the area.
- Immediately shut off the hydrogen source.
- Provide adequate ventilation to clear the affected area.

Fire or explosion

- Immediately shut off the hydrogen source.
- Report the fire and follow the fire response procedures for the laboratory.
- Leave escaping hydrogen to "burn down". **Note: The flame of burning hydrogen is not highly visible.**
- Use a class D fire extinguisher or dry sand to extinguish burning metal hydride powder. If smouldering metal hydride powder cannot ignite adjacent materials, it may be best to leave the hydride burning. **Note: Do not use water or CO₂ extinguishers.**

Other emergencies not involving hydrogen escape

Immediately switch off the FC50, remove its hydrogen connecting tube and if necessary close the valve of the metal hydride storage canister.



Australian Government
 Department of Defence
 Defence Science and
 Technology Organisation

WorkingSAFER RISK ASSESSMENT REPORT

Initial Assessment Date 22/02/2010

Last Updated Date 23/08/2011

Next Review Date Not set

Assessment Number	1272	Version	1
Assessment Title	*ARCHIVED* Operation of 50W PEM Fuel Cell		
Assessment Description	<p>A 50 W proton exchange membrane fuel cell which uses hydrogen gas as a fuel and laboratory air as an oxidant has been purchased from Hellocentris (Germany). The fuel cell ,associated loads and power supplies which are designed for educational and research purposes come in modular form and have been assembled on a mounting frame supplied by the manufacturer. The completed assembled package is housed in the operational and regularly certified fume hood in Room M2.76 of Building 94.</p> <p>Hydrogen gas used to power the fuel cell is stored in the form of a stable metal hydride powder which is housed in a small aluminium canister. The canister, weighing approximately 2 kg, is filled with ultra high purity hydrogen gas stored in a Size D cylinder located in MPDs gas cylinder holding store situated outside Building 94. The charge weight of hydrogen is typically 22 g. Safety aspects of this filling activity are covered in Assessment 1193. Operation of the fuel cell is under the control of an onboard microcomputer which monitors hydrogen flow rate, cell temperature and air flow.</p>		
Principal Risk Assessor	Kane Ivory		
Risk Assessment Contributors	Stuart Riddell, James Harvey, Michael Newman, Steven Pas		
Approver Name	Gaylor, Kevin		
Approver Comment			
Approval Status	Draft		
Approval Date			
Laboratory/Division	PR&HS - 1000010	MPD - 1000104	
State/Territory	VIC		
Assessment Commencement Date	27/07/2009		
Environment	Laboratory M2.76 of Building 94		
Equipment	The 50W PEM Fuel Cell system consists of the Fuel Cell Module FC50 (including power supply, control software, documentation), the Electronic Load Module EL200, the Voltage Converter Module VC100 and Ovonic's 2.2 kg Metal Hydride storage canister with refilling kit.		
Personnel	One person with appropriate training and background is to be present at all times during the fuel cell's operation. The required training/experience includes the operation of the fuel cell system itself and competence in dealing with small fires using portable fire extinguishers.		

HAZARDS ASSOCIATED WITH ASSESSMENT - 1272 , VERSION 1

RATINGS

1. HAZARD:	ERGONOMICS /Office workstation/desk top	
Controls	<p>HAZARD DETAILS Sitting at the desk and using the Fuel Cell system</p> <p>CONTROLS - ELIMINATE N/A</p> <p>CONTROLS - SUBSTITUTE N/A</p> <p>CONTROLS - ENGINEERING N/A</p> <p>CONTROLS - ADMINISTRATIVE - The workstation shall be setup to conform with the ergonomic checklist that can be found on DSTO OHS website. Where this is not possible, concerns shall be raised within PES group and mitigation activities shall be undertaken. - Operators shall take regular breaks from sitting at the desk.</p> <p>CONTROLS - PPE N/A</p>	
Likelihood	<p>LIKELIHOOD - NO CONTROLS: UNLIKELY Poor posture for an extended period could lead to stress on the body, but would not be considered a regular or likely occurrence.</p> <p>LIKELIHOOD - USING CONTROLS: RARE Proper adherence to the controls makes the probability of an incident negligible.</p>	Rare
Consequences	<p>CONSEQUENCE - NO CONTROLS: MODERATE Potential for consequences such as back or repetitive strain injuries.</p> <p>CONSEQUENCE - USING CONTROLS: MINOR Extent of injuries described above will be reduced.</p>	Minor
Risk Rating	<p>RISK RATING NO CONTROLS: MODERATE USING CONTROLS: LOW</p> <p>Manage by routine procedures</p>	Low

2. HAZARD:	HUMAN FACTORS /Manual handling	
Controls	<p>HAZARD DETAILS Moving and handling the fuel cell system which is on a large display stand.</p> <p>CONTROLS - ELIMINATE N/A</p> <p>CONTROLS - SUBSTITUTE N/A</p> <p>CONTROLS - ENGINEERING - Heliocentris' Hy-Expert Instructor Fuel Cell System is arranged in a frame, which can be disassembled for ease of transport. The arrangement within the frame allows the system to be set up in a convenient manner such that the operator can make modifications with minimal effort.</p> <p>CONTROLS - ADMINISTRATIVE - If the system needs to be moved, 2 or more staff will be used to lift the system. - Alternatively, the system will be disassembled and moved one piece at a time.</p> <p>CONTROLS - PPE - Safety boots with steel caps shall be worn whenever manual handling activities are being conducted. - At all times, shoes with enclosed toes shall be worn.</p>	
Likelihood	<p>LIKELIHOOD - NO CONTROLS: UNLIKELY The fuel cell system is constructed in a user friendly frame, which once constructed requires little modification. Therefore, major modifications, excluding connecting and disconnecting the metal hydride canister, would be relatively infrequent.</p> <p>LIKELIHOOD - USING CONTROLS: RARE Proper adherence to the controls makes the probability of an incident negligible.</p>	Rare
Consequences	<p>CONSEQUENCE - NO CONTROLS: MODERATE Incorrect handling procedures could lead to back damage.</p> <p>CONSEQUENCE - USING CONTROLS: MINOR Adherence to controls should limit potential injury to minor finger or wrist damage.</p>	Minor

Risk Rating	Manage by routine procedures	Low
3. HAZARD:	HUMAN FACTORS /Working alone	
Controls	<p>HAZARD DETAILS Working alone in the lab while operating the fuel cell system. NOTE: Working alone is not considered a direct hazard, and is instead considered to magnify other hazards. Such hazards have been assessed under the context of working alone where appropriate.</p> <p>CONTROLS - ELIMINATE N/A</p> <p>CONTROLS - SUBSTITUTE N/A</p> <p>CONTROLS - ENGINEERING - The Fuel Cell system is installed with software that shuts the system down automatically in the event of an error, which could potentially be dangerous or damaging to the system. Such errors include lack of hydrogen supply, over heating, load current too high, leaking in system, etc.</p> <p>CONTROLS - ADMINISTRATIVE - The PES group 'Working alone' guidelines shall be followed. - Another PES group member shall be notified in advance. - Other group members shall periodically check on person working alone. - Lab door shall be unlocked whenever someone is present in the lab. - Personnel shall be members of the PES group who know how to use the system, and shall be familiar with this risk assessment, the standard operating procedure for the system, and with the experimental procedure for the activity they are conducting.</p> <p>CONTROLS - PPE N/A</p>	
Likelihood	NOTE: Working alone is not a direct hazard, and as such is not viewed to have a directly associated likelihood, consequence or risk rating. As a result they have all been left as the default, 'Not Assigned'.	Not Assigned
Consequences	See note in 'Likelihood' section.	Not Assigned
Risk Rating	The likelihood and/or consequence rating has yet to be selected - please complete	Not Determined
4. HAZARD:	MECHANICAL /Kinetic	
Controls	<p>HAZARD DETAILS The cooling/oxygen supply fans are small ~0.6W ducted fans however they may impact on fingers causing minor injury.</p> <p>CONTROLS - ELIMINATE N/A</p> <p>CONTROLS - SUBSTITUTE N/A</p> <p>CONTROLS - ENGINEERING - The ducts themselves act as protective barriers, which reduce the likelihood of fingers impacting with the fan blades.</p> <p>CONTROLS - ADMINISTRATIVE N/A</p> <p>CONTROLS - PPE N/A</p>	
Likelihood	<p>LIKELIHOOD - NO CONTROLS: RARE The use of relatively low power ducted fans minimises the risk of injury caused by impact to the operators limbs</p> <p>LIKELIHOOD - USING CONTROLS: RARE No control other than design of rig implemented.</p>	Rare
Consequences	<p>CONSEQUENCE - NO CONTROLS: MINOR Cut to finger from impact with fan blade.</p> <p>CONSEQUENCE - USING CONTROLS: MINOR Unable to reduce consequence</p>	Minor
	<p>RISK RATING NO CONTROLS: LOW</p>	

	USING CONTROLS: LOW	
Risk Rating	Manage by routine procedures	Low
<hr/>		
5. HAZARD:	MECHANICAL /Pressure (gas/liquid)	
Controls	<p>HAZARD DETAILS Leakage of hydrogen from the transfer line connecting the fuel cell to the hydride canister may occur. One of the safety features of metal hydride gas storage is that should a rupture of the canister occur an instantaneous release of gas at high pressure does not take place. This evolves from the deposition of hydrogen into a metal lattice and the need for the application of heat for an endothermic desorption process to take place. Leakage of gas, therefore, tends to be self limiting unless a considerable amount of heat is applied.</p> <p>CONTROLS - ELIMINATE N/A</p> <p>CONTROLS - SUBSTITUTE N/A</p> <p>CONTROLS - ENGINEERING N/A</p> <p>CONTROLS - ADMINISTRATIVE - Regular inspections and the application of a leak detecting solution is expected to reduce the likelihood of this occurring.</p> <p>CONTROLS - PPE - Safety glasses and appropriate clothing are to worn to minimise injury caused by escaping gas at high pressure.</p>	
Likelihood	<p>LIKELIHOOD - NO CONTROLS: POSSIBLE</p> <p>LIKELIHOOD - USING CONTROLS: UNLIKELY Regular checking of gas lines, cylinder pressure regulators and unions for integrity and performance should ensure that the likelihood of hydrogen gas leakage is minimal.</p>	Unlikely
Consequences	<p>CONSEQUENCE - NO CONTROLS: MODERATE Injury to eyes from escaping gas at high pressure.</p> <p>CONSEQUENCE - USING CONTROLS: MINOR Use of PPE reduces extent of likely injuries.</p> <p>RISK RATING NO CONTROLS: HIGH USING CONTROLS: LOW</p>	Minor
Risk Rating	Manage by routine procedures	Low
<hr/>		
6. HAZARD:	ELECTRICAL /Energised electrical equipment	
Controls	<p>HAZARD DETAILS Heliocentris' Hy-Expert Instructor Fuel Cell System is connected to the 240V AC mains via a 12V DC power supply.</p> <p>CONTROLS - ELIMINATE N/A</p> <p>CONTROLS - SUBSTITUTE N/A</p> <p>CONTROLS - ENGINEERING - The electronics are contained within the system's frame, and little manipulation of its electronics is required by the operator, with the exception of plugging in/unplugging leads. In addition, relatively low voltage equipment and well insulated plugs and leads are utilised.</p> <p>CONTROLS - ADMINISTRATIVE - The polarity of the system's electrical connections are clearly labelled with '+' and '-' symbols and are appropriately colour coded.</p> <p>CONTROLS - PPE N/A</p>	
Likelihood	<p>LIKELIHOOD - NO CONTROLS: RARE The nature of the Hy-Expert fuel cell system's design significantly reduces the probability of electric shock to the operator.</p> <p>LIKELIHOOD - USING CONTROLS: RARE</p>	Rare
Consequences	<p>CONSEQUENCE - NO CONTROLS: CATASTROPHIC In the worst case, an incident with energise electrical equipment could lead to death.</p>	Catastrophic

CONSEQUENCE - USING CONTROLS: CATASTROPHIC
 Controls can not reduce consequence of this hazard.

RISK RATING
 NO CONTROLS: HIGH
 USING CONTROLS: HIGH

Risk Rating **Senior management approval required - monitor closely** **High**

7. HAZARD: **ELECTRICAL /Ignition sources**

Controls
 HAZARD DETAILS
 Hydrogen gas can be ignited by several sources including static charge, hot surfaces, electrical sparks and flames. Although the fuel cell will be warm during operation this temperature will be insufficient to cause autoignition of leaking hydrogen gas. As the fuel cell will be operated in a laboratory where smoking is prohibited and welding operations require specific permission it is unlikely that either of these ignition sources would be present.

CONTROLS - ELIMINATE
 N/A

CONTROLS - SUBSTITUTE
 N/A

CONTROLS - ENGINEERING
 - The case of the power supply is earthed to mains to reduce the risk of any static charge build up.

CONTROLS - ADMINISTRATIVE
 - Personnel who could potentially carry ignition sources will be kept well away from the area by barrier poles and warning signs.

CONTROLS - PPE
 N/A

Likelihood **LIKELIHOOD - NO CONTROLS: UNLIKELY** **Unlikely**
 IT is possible for a static shock to occur, although due to grounding of power supply this is considered unlikely to occur.

LIKELIHOOD - USING CONTROLS: RARE
 The use of the previously mentioned preventive controls should reduce the likelihood of an ignition source entering the vicinity of the hydrogen canister. In addition, the use of ceiling ventilation should remove any leaking hydrogen from the laboratory. Therefore, the chances of igniting the hydrogen gas is unlikely.

Consequences **CONSEQUENCE - NO CONTROLS: MODERATE** **Moderate**
 Ignition sources in the presence of leaking hydrogen gas could cause a minor fire.

CONSEQUENCE - USING CONTROLS: MODERATE
 Controls can not reduce consequences of hazard.

RISK RATING
 NO CONTROLS: MODERATE
 USING CONTROLS: MODERATE

Risk Rating **Line management approval required - consider further risk reduction measures** **Moderate**

8. HAZARD: **THERMAL /Hot substances**

Controls
 HAZARD DETAILS
 Potential thermal hazard from the fuel cell stack.

CONTROLS - ELIMINATE
 N/A

CONTROLS - SUBSTITUTE
 N/A

CONTROLS - ENGINEERING
 - The temperature of the fuel cell stack is not expected to exceed 50°C as the Hy-Expert incorporates an emergency fail safe, which autonomously shuts down the system when the stack temperature exceeds 50°C. Furthermore, given that the fuel cell stack is conveniently attached to the Hy-Expert frame, little manual handling is required by the operator during operation.

CONTROLS - ADMINISTRATIVE
 N/A

CONTROLS - PPE
 N/A

Likelihood **LIKELIHOOD - NO CONTROLS: UNLIKELY** **Unlikely**
 The Hy-Expert's fail safe mechanism prevents the fuel cell stack

	from exceeding 50°C. Therefore, the likelihood of burn injuries being suffered by the operator is unlikely.	
	LIKELIHOOD - USING CONTROLS: UNLIKELY No further controls other than design of the rig implemented	
Consequences	CONSEQUENCE - NO CONTROLS: MINOR	Insignificant
	CONSEQUENCE - USING CONTROLS: INSIGNIFICANT Burns could result from over heated fuel cell stack, though thermal cut out would prevent temperature from being greater than 50°C.	
	RISK RATING NO CONTROLS: LOW USING CONTROLS: LOW	
Risk Rating	Manage by routine procedures	Low

9. HAZARD:	THERMAL /Fire / flames	
Controls	HAZARD DETAILS A fire starting in the laboratory could originate from the ignition of hydrogen gas or the solid metal hydride material contained in the 1.2 kg vessel. CONTROLS - ELIMINATE N/A CONTROLS - SUBSTITUTE N/A CONTROLS - ENGINEERING N/A CONTROLS - ADMINISTRATIVE N/A CONTROLS - PPE - For a fire involving the burning of hydrogen only a portable carbon dioxide fire extinguisher will be used. This extinguisher has been procured and will be positioned conveniently within the laboratory. For a fire involving the combustion of the pyrophoric metal hydride the use of a carbon dioxide or water based extinguishing agent is prohibited and a 9 kg Class D fire extinguisher has been purchased and will be used to deal with this contingency. The Class D extinguisher will also be positioned in a convenient location within the laboratory. A 10 litre bucket of dry sand will be located nearby and will be used as a smothering agent for a fire involving the burning of either hydrogen gas or metal hydride. The dry sand will also be used to contain and prevent the ignition of the metal hydride powder in the situation where the canister is dropped and ruptured causing the contents to be dispersed.	
Likelihood	LIKELIHOOD - NO CONTROLS: UNLIKELY Fire requires both leaking of hydrogen gas and an ignition source. LIKELIHOOD - USING CONTROLS: RARE The likelihood of a fire occurring is minimized by adopting controls which are related to gas leakage and ignition sources. Should these controls not prove to be effective suitable fire fighting equipment is available.	Rare
Consequences	CONSEQUENCE - NO CONTROLS: MODERATE Ignition of leakign hydrogen gas could cause a minor fire. CONSEQUENCE - USING CONTROLS: MODERATE Controls can not reduce consequences of hazard.	Moderate
	RISK RATING NO CONTROLS: MODERATE USING CONTROLS: MODERATE	
Risk Rating	Line management approval required - consider further risk reduction measures	Moderate

The following hazards have a risk rating of moderate or higher

Additional controls will need to be considered and factored into the relevant risk assessment to be conducted in the lab, workshop, field, trial, etc before commencement of work

HIGHER RISK HAZARDS FOR ASSESSMENT - 1272 , VERSION 1

RESULTANT RISK RATING

1.ELECTRICAL/Energised electrical equipment	High
2.ELECTRICAL/Ignition sources	Moderate
3.THERMAL/Fire / flames	Moderate

DEFENCE SCIENCE AND TECHNOLOGY ORGANISATION DOCUMENT CONTROL DATA				1. PRIVACY MARKING/CAVEAT (OF DOCUMENT)	
2. TITLE The Characterisation of a PEM Fuel-Cell System with a Focus on UAS Applications			3. SECURITY CLASSIFICATION (FOR UNCLASSIFIED REPORTS THAT ARE LIMITED RELEASE USE (L) NEXT TO DOCUMENT CLASSIFICATION) Document (U) Title (U) Abstract (U)		
4. AUTHOR(S) James R. Harvey and Jennifer L. Palmer			5. CORPORATE AUTHOR DSTO Defence Science and Technology Organisation 506 Lorimer St Fishermans Bend Victoria 3207 Australia		
6a. DSTO NUMBER DSTO-TR-2934		6b. AR NUMBER AR-015-844		6c. TYPE OF REPORT Technical Report	
				7. DOCUMENT DATE January 2014	
8. FILE NUMBER 2012/1145535/1	9. TASK NUMBER 07/292		10. TASK SPONSOR Chief Defence Scientist	11. NO. OF PAGES 58	
				12. NO. OF REFERENCES 92	
13. DSTO Publications Repository http://dspace.dsto.defence.gov.au/dspace/			14. RELEASE AUTHORITY Chief, Aerospace Division		
15. SECONDARY RELEASE STATEMENT OF THIS DOCUMENT <i>Approved for public release</i> OVERSEAS ENQUIRIES OUTSIDE STATED LIMITATIONS SHOULD BE REFERRED THROUGH DOCUMENT EXCHANGE, PO BOX 1500, EDINBURGH, SA 5111					
16. DELIBERATE ANNOUNCEMENT No Limitations					
17. CITATION IN OTHER DOCUMENTS Yes					
18. DSTO RESEARCH LIBRARY THESAURUS Unmanned aircraft system, unmanned aerial vehicle, aircraft performance, fuel cell, fuel-cell stack, electric propulsion, hybrid propulsion, electrical power					
19. ABSTRACT Under DSTO's Strategic Research Initiative on Signatures, Materials, and Energy, a project entitled "Hybrid-Propulsion and Power-Management Technologies for Tactical Unmanned Aircraft Systems (UAS)" is underway. In this project, fuel cells have been identified as having the potential to substantially increase the range and endurance of small, electrically-powered fixed-wing aircraft. Herein described are experiments conducted on a Hy-Expert Instructor Fuel Cell System, aimed at developing fundamental knowledge of PEM fuel-cell characteristics and the methodology used to characterise fuel-cell systems. Given the focus of future work, emphasis was placed on issues relevant to UAS applications.					